Functional susceptibility of tropical forests to climate change

Aguirre-Gutiérrez, J., Berenguer, E., Oliveras Menor, I. [et al.]

DOI:
https://doi.org/10.1038/s41559-022-01747-6

ARTICLES
https://doi.org/10.1038/s41559-022-01747-6

nature ecology & evolution

Check for updates

Functional susceptibility of tropical forests to climate change

Jesús Aguirre-Gutiérrez[1,2]✉, Erika Berenguer[1,3], Imma Oliveras Menor[1,4], David Bauman[1,4,5], Jose Javier Corral-Rivas[6], Maria Guadalupe Nava-Miranda[7], Sabine Both[8], Josué Edzang Ndong[9], Fidèle Evouna Ondo[9], Natacha N'ssi Bengone[10], Vianet Mihinhou[10], James W. Dalling[11,12], Katherine Heineman[12], Axa Figueiredo[13], Roy González-M[14], Natalia Norden[14], Ana Belén Hurtado-M[14], Diego González[14], Beatriz Salgado-Negret[15], Simone Matias Reis[1,16], Marina Maria Moraes de Seixas[17], William Farfan-Rios[18,19,20], Alexander Shenkin[1], Terhi Riutta[1,21], Cécile A. J. Girardin[1], Sam Moore[1], Kate Abernethy[22,23], Gregory P. Asner[24], Lisa Patrick Bentley[25], David F.R.P. Burslem[26], Lucas A. Cernusak[27], Brian J. Enquist[28], Robert M. Ewers[29], Joice Ferreira[30], Kathryn J. Jeffery[29], Carlos A. Joly[31], Ben Hur Marimon-Junior[16], Roberta E. Martin[24], Paulo S. Morandi[16], Oliver L. Phillips[32], Amy C. Bennett[32], Simon L. Lewis[32,33], Carlos A. Quesada[34], Beatriz Schwantes Marimon[16], W. Daniel Kissling[35], Miles Silman[36], Yit Arn Teh[37], Lee J. T. White[10,22,23], Norma Salinas[38], David A. Coomes[39], Jos Barlow[3], Stephen Adu-Bredu[40] and Yadvinder Malhi[12]

Tropical forests are some of the most biodiverse ecosystems in the world, yet their functioning is threatened by anthropogenic disturbances and climate change. Global actions to conserve tropical forests could be enhanced by having local knowledge on the forests' functional diversity and functional redundancy as proxies for their capacity to respond to global environmental change. Here we create estimates of plant functional diversity and redundancy across the tropics by combining a dataset of 16 morphological, chemical and photosynthetic plant traits sampled from 2,461 individual trees from 74 sites distributed across four continents together with local climate data for the past half century. Our findings suggest a strong link between climate and functional diversity and redundancy with the three trait groups responding similarly across the tropics and climate gradient. We show that drier tropical forests are overall less functionally diverse than wetter forests and that functional redundancy declines with increasing soil water and vapour pressure deficits. Areas with high functional diversity and high functional redundancy tend to better maintain ecosystem functioning, such as aboveground biomass, after extreme weather events. Our predictions suggest that the lower functional diversity and lower functional redundancy of drier tropical forests, in comparison with wetter forests, may leave them more at risk of shifting towards alternative states in face of further declines in water availability across tropical regions.

Tropical forests are amongst the most biodiverse ecosystems on the planet[1]; they harbour more than 50% of global biodiversity including between 67% and 88% of all tree species and are responsible for more than 30% of terrestrial productivity[2,3]. Given the large distribution of tropical forests on earth, small but widespread changes in their tree community composition can have global impacts in the removal of CO_2 from the atmosphere[4]. Tropical forests are also essential to help mitigate the effects of climate change, as intact tropical forests are carbon sinks of around 1.26 Pg C per year[5]. However, carbon storage can be negatively impacted by changes in water availability[6]. For example, the Amazon forest, which contains close to 123 Pg C of above and belowground biomass[7] lost 1.2 Pg–1.6 Pg C (ref. [8])—the equivalent of 1% of its total carbon stocks[9]—during the extreme drought of 2005 and it is now suggested to be a carbon source[10]. Besides impacting the carbon storage capacity of forests, changes in climate mean states and variability are key potential drivers of biodiversity declines around the world[11,12]. Understanding how climate may affect tropical forests' capacity to store carbon thereby requires evaluation of how plants respond to drought stress. To do so, the Maximum Climatic Water Deficit (MCWD) and Vapour Pressure Deficit (VPD) are two fundamental proxies of hydric stress for plants[13,14], with increases in VPD leading to greater plant transpiration stress[15,16] (Costa et al. provide a review on the water table depth as another highly relevant metric under drought[17]). Although it has been generally expected that communities historically adapted to high MCWD and VPD should be better adapted to increasing drier conditions, it could also be that such communities might already be at their climatic physiological limits and thus further droughts may increase water stress to such an extent that they are driven towards alternative states[18,19]. To disentangle these two possibilities, evaluating functional trait composition may provide clues on their possible historical adaptations

A full list of affiliations appears at the end of the paper.

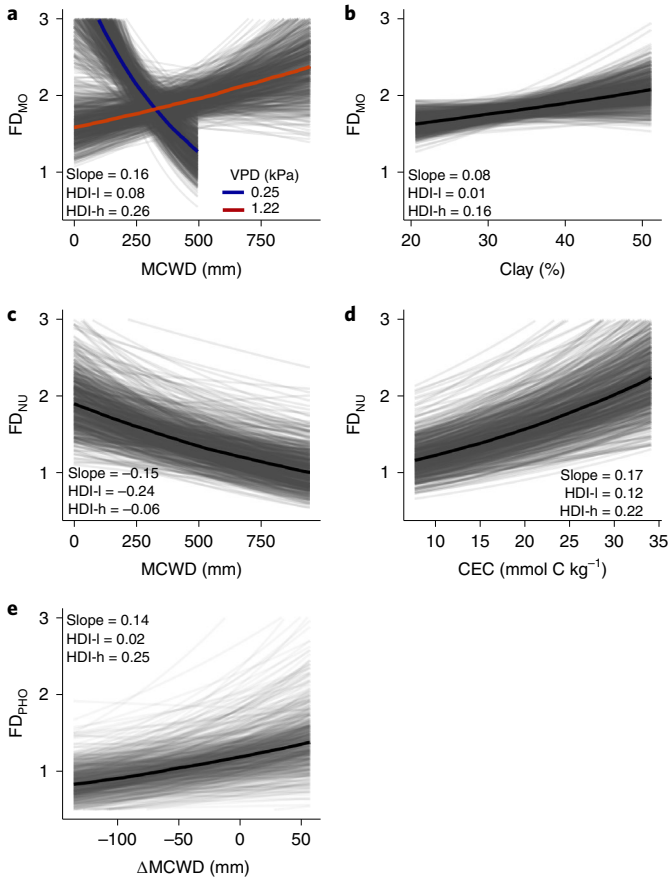

Fig. 1 | Long-term water availability and its recent changes and soil conditions drive FD of plant traits across the tropics. a–e, Model results for FD of morphological (**a**,**b**), leaf nutrient (**c**,**d**) and photosynthetic (**e**) traits are shown. Only climatic variables (*x* axis) with a clearly important relationship (90% HDI of the posterior distribution does not overlap 0) with FD are shown. Models for each group (morphology/structure, leaf nutrients, photosynthetic) were fitted as a function of long-term and recent changes in climate and of soil chemistry (CEC) and texture (clay). Thick black lines show the average response, and shaded lines show 300 random draws from the model posterior distribution representing variability of the expected model fit. The blue fitted line in **a** shows the effect of MCWD at the lowest value of VPD, and the red fitted line shows the effect of MCWD at the highest value of VPD. Larger positive values in MCWD and VPD reflect stronger water deficits. The *y* axis shows the FD of morphological/structural (FD_{MO}), leaf nutrient (FD_{NU}) and photosynthetic (FD_{PHO}) traits. HDI-l, highest density interval (lowest bound); HDI-h, highest density interval (highest bound). Supplementary Table S1 provides details about the single traits that form each of the groups (morphology/structure, leaf nutrients, photosynthetic). Supplementary Table S3 provides full statistical results.

to water stress conditions[20,21]. Although changes in MCWD and VPD are prominent features of climate change across tropical forests, detailed analyses that show their relationship with plant morphology/structure, leaf chemistry and photosynthesis-related traits across climatic and elevation gradients at a pantropical scale remain scarce. Thus, understanding the functional climatic gradients relationship is key to disentangling the long-term role of tropical forests for mitigating climate change and is crucial for deciphering the resilience of key ecosystem properties such as diversity and carbon stocks under a changing climate.

Ecosystem resilience may increase through different pathways, for example, by species having the same traits that affect a given ecosystem process, such as carbon capture, but different traits to respond to environmental changes, such as droughts. Arguably functional traits may respond differently to diverse drivers of change (for example, temperature or precipitation change), which may be reflected in trait diversity but not necessarily in species richness[22] given that there is not always a tight relation between species richness and functional trait diversity[23,24]. According to the biodiversity–ecosystem functioning insurance hypothesis[25], ecosystem functions should be less affected by a changing environment when (1) the ecosystem possesses both high functional diversity (for example, large range of trait values; FD), (2) but also a wide set of species with similar functional characteristics[23], conferring the system with high functional redundancy (FRed)[26,27]. Thus, in communities with high FD and high FRed, the loss of a given species is less likely to result in the disruption of the ecosystem function[28] as other species will probably continue carrying out the same functions, compensating the lost species[29,30]. High FD and high FRed may enhance the temporal stability of ecosystem functions (for example, biomass productivity)[31] and thus provide a buffering effect against environmental changes[25], conferring higher resilience. Nonetheless, these hypotheses have never been tested across the tropics, and the role of FD and FRed for maintaining the tropical forests' ability to capture and store carbon remains to be tested and quantified at this global scale. Quantifying the FD and FRed is crucial to advancing our understanding of the resilience of these forests in the Anthropocene.

Here we address this knowledge gap by combining a new pantropical dataset of 16 plant traits related to morphology/structure (leaf area, leaf dry and fresh mass, leaf dry matter content, leaf water content, specific leaf area (SLA), leaf thickness, wood density), foliar nutrients (leaf calcium, potassium, magnesium, nitrogen and phosphorus content) and photosynthesis (photosynthetic rate, dark respiration). These plant traits are hypothesized to be of importance for tropical forests to adapt or respond to a drying climate (Supplementary Table S1 provides a description of their hypothesized importance). The importance of such traits relies on their influence on the capacity of species to capture energy for growth and conserve resources (for example, water) for survival under stressful environmental conditions such as droughts and have been shown to change in response to a changing climate[20,32,33]. The plant traits were collected from 2,461 individual trees belonging to 1,611 species distributed across 74 plots that contained 32,464 individual trees equal to or greater than 10 cm diameter at breast height from 2,497 species (Extended Data Fig. 1, Supplementary Table S2 and Methods). The vegetation plots are free of obvious local anthropogenic disturbance (that is, far from forest edges and no evidence of logging or fires) and cover a wide range of the climatic conditions found across tropical and subtropical dry and moist broadleaf forests (Extended Data Figs. 2 and 3). This dataset was combined with estimates of MCWD and VPD from 1958 to 2017 and of soil chemistry (cation exchange capacity) and texture (clay content) (Extended Data Fig. 3).

We address three fundamental questions: (1) does the long-term mean ambient water stress environment (MCWD and VPD) or its changes (ΔMCWD and ΔVPD) over the past half century determine current functional diversity (Extended Data Fig. 3)? First, we examine the relationship between the FD (calculated here as functional dispersion[34]) and FRed levels across tropical regions. The relationship between changes in climate and long-term FD and FRed can be understood as a proxy of the effects of climate change on the functional diversity levels of the ecosystem given that we do not quantify their direct effect on changes in FD and FRed. (2) What is the spatial distribution of FD and FRed across tropical forests? (3) Is there a relationship between FD or FRed and one metric of ecosystem functioning (aboveground biomass) during extreme drought events? We expect that: (1) communities that are found in drier climate conditions and that have experienced stronger

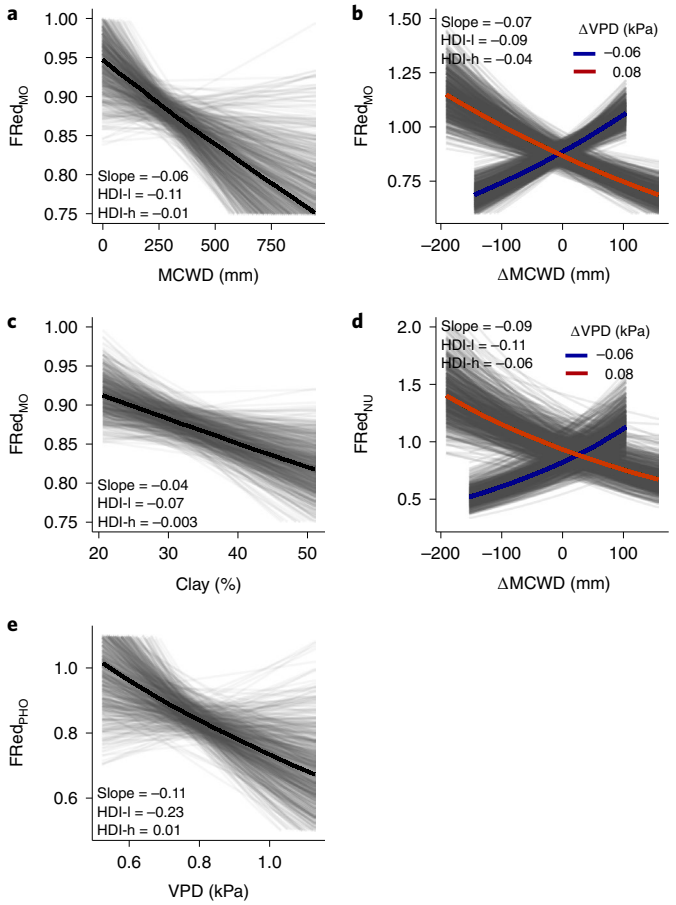

Fig. 2 | Long-term water availability and its recent changes and soil texture drive FRed of plant traits across the tropics. a–e, Model results for FRed of morphological (**a**–**c**), leaf nutrient (**d**) and photosynthetic (**e**) traits are shown. Only climatic variables (*x* axis) with a clearly important relationship (90% HDI of the posterior distribution does not overlap 0) with FRed are shown except in **e** where the effect of VPD on $FRed_{PHO}$ is marginal. Models for each group (morphology/structure, leaf nutrients, photosynthetic) were fitted as a function of long-term changes in climate and of soil chemistry (CEC) and texture (clay). Thick black lines show the average response, and shaded lines show 300 random draws from the model posterior distribution representing variability of the expected model fit. The blue fitted line in **b** and **d** shows the effect of ΔMCWD at the largest decrease in ΔVPD and the red fitted line at the larger increase in ΔVPD. Larger positive values in MCWD reflect stronger water deficits. The *y* axis shows the FRed of morphological/structural ($FRed_{MO}$), leaf nutrient ($FRed_{NU}$) and photosynthetic ($FRed_{PHO}$) traits. Supplementary Table S1 provides details about the single traits that form each of the groups (morphology/structure, leaf nutrients, photosynthetic). Supplementary Table S3 shows full statistical results.

decreases in water availability across the past half century will be less functionally diverse but may be more functionally redundant as a result of climate filtering for better-adapted traits than communities in less extreme conditions such as wetter forests; (2) across the full spatial distribution of tropical forests, tropical wet forest communities, which are more species rich than drier tropical forests, have higher FD given a broader set of ecological strategies available as a result of more stable and favourable climate; (3) there is a positive relationship among FD, FRed and ecosystem functioning (that is, aboveground biomass) as more functionally diverse and redundant communities may attenuate the negative effects of a changing climate and may therefore be considered to be more resilient.

Results

FD, FRed and forest susceptibility. Fundamental knowledge on the climate–FD and climate–FRed relationships across tropical forest ecosystems has been missing. To fill this knowledge gap, we calculated for vegetation plots distributed across the tropics the FD and FRed for morphological/structural, leaf chemistry and photosynthetic traits that are hypothesized to be of importance for tropical forests to respond to a drying climate. The selected traits play a role in plant establishment, growth and/or survival[20,21,35] (Supplementary Table S1). Then, we investigated variation in FD and FRed across tropical forests by modelling their relation with MCWD, VPD and their interaction and the ΔMCWD and ΔVPD and their interaction (Methods), where more positive values in MCWD and VPD reflect stronger water deficits. In our models, we also accounted for soil characteristics (Methods) such as texture (clay percentage) and chemistry (cation exchange capacity, CEC). Soils high in clay content may have high water-holding capacity over longer periods of time, which is important for vegetation under drought conditions[32]. Moreover, it is widely acknowledged that tropical forests in drier regions are generally associated with soils that are richer in nutrients in comparison with wet tropical forests[36]. The feedbacks between soil and rainfall and their effects on plant distributions could be disrupted under a changing climate and therefore have adverse effects on the functioning of tropical forest ecosystems. A principal component analysis (PCA) of climate conditions (long-term trends and recent changes) indicated that the first two axes explained 71.3% of the variation among plots (Extended Data Fig. 4a) and the first two axes of the soil-based PCA (with soil chemistry and texture) account for 83% of the variation among plots (Extended Data Fig. 4b).

On the basis of the long-term mean MCWD, our results show that drier tropical forests are clearly morphologically less diverse (slope = −0.18 [−0.31, −0.05], median and 90% highest density intervals) than wet forests (Supplementary Table S2). The effect of MCWD on morphological FD was modulated by atmospheric VPD, where the FD of communities with low VPD (blue fitted line in Fig. 1a) strongly decreased as MCWD increased, but FD tended to increase with MCWD in communities where VPD was high (red fitted line in Fig. 1a). Morphological/structural FD increased linearly with increases in clay content (slope = 0.08 [0.01, 0.16]; Fig. 1b). Foliar nutrients' FD also tended to decrease towards drier forests (slope = −0.15 [−0.24, −0.05]; Fig. 1c). Overall, foliar nutrients' FD increased towards communities with higher soil CEC (slope = 0.17 [0.12, 0.22]; Fig. 1d), while photosynthetic FD also increased towards areas that experienced stronger increases in MCWD (slope = 0.14 [0.02, 0.25]; Fig. 1e) but did not respond to the long-term mean MCWD. For the trait groups (morphology, nutrients, photosynthesis) for which a clear relationship with climate and soil was found (90% highest density interval, HDI, of the posterior distribution does not overlap 0; Supplementary Table S3), the models explained (R^2) 44%, 75% and 75% of the variation in morphology/structure, nutrients and photosynthetic FD, respectively.

The models of FRed as a function of climate and soil explained 53%, 73% and 33% of the variation in morphology/structure, nutrients and photosynthetic FRed, respectively, across the tropical forest. The FRed models (Supplementary Table S3) showed that redundancy of morphological/structural (slope = −0.06 [−0.11, −0.01]) traits declines with higher long-term mean MCWD and that photosynthetic FRed declines as long-term VPD increases (slope = −0.11 [−0.23, −0.01]; Fig. 2a,e, respectively). While redundancy of morphological/structural and foliar nutrient traits decreased with increases in MCWD through time (ΔMCWD) in areas that also increased the most in VPD (ΔVPD; Fig. 2b,d red fitted line), the opposite was predicted for areas that experienced larger increases in MCWD but smaller increases in VPD (Fig. 2b,d blue fitted line). FRed of morphological/structural traits also tended

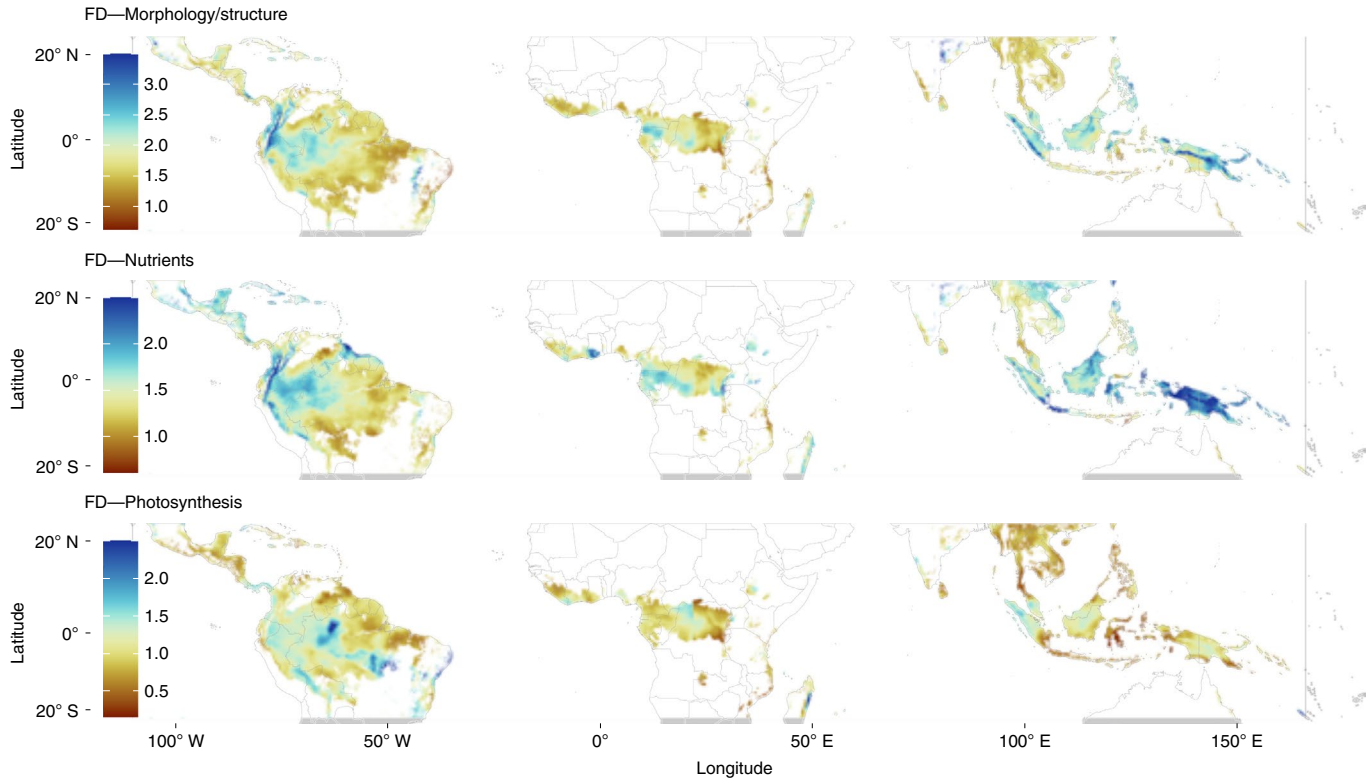

Fig. 3 | Global predictions of FD across the tropical and subtropical dry and moist broadleaf forests. FD predictions for morphological/structural (top panel), leaf nutrient (middle panel) and photosynthetic (bottom panel) traits are shown. Dark brown colours depict areas where FD is lowest, light brown and light blue where FD is intermediate and dark blue where FD is predicted to be highest. FD predictions across the tropics were made using the statistical models for which details are shown in Supplementary Table S3. The locations of field sites that provided data that informed this analysis are shown in Supplementary Fig. S5.

to decrease with increases in soil clay content (slope = −0.04 [−0.07, −0.003]; Fig. 2c).

Mapping FD and FRed. On the basis of our understanding of the relation of FD and FRed of morphological/structural, leaf nutrient and photosynthetic trait groups with climate and soil (Figs. 1 and 2) and to fill the knowledge gap on the pantropical distribution of FD and FRed, we created pantropical maps of both FD (Fig. 3) and FRed (Fig. 4) distribution. With our map predictions, we aim to uncover the locations of forests with potentially higher and lower resilience to a changing climate. To this end, we used the statistical models built above (Supplementary Table S3) to predict FD and FRed across the pantropical dry and moist broadleaf forests for which our field-sampling locations have a wide representation of the climatic conditions across those tropical forests (Extended Data Figs. 2, 5 and 6). On the basis of the FD and FRed predictions, we calculated the percent area that had 'low', 'intermediate' and 'high' diversity and redundancy for each trait group (Methods). We also created bivariate maps that combine the FD and FRed scores in a single map to visualize where FD and FRed are both maximized and minimized across the tropics (Fig. 5). We further developed the same statistical models as described above but removed from the analysis all plots from each continent (Asia and Australia out at the same time) to determine which regions have a higher contribution to determining the observed spatial predictions (those of Fig. 5). For morphology/structure, foliar nutrients and photosynthesis, we found high correlations between the bivariate maps developed with the full dataset and when Asia and Australia were left out (r = 0.96, 0.82 and 0.94; Extended Data Figs. 7, 8 and 9, respectively, and Supplementary Fig. 1). For morphology/structure and photosynthesis, there were also high correlations between the patterns based on the full dataset and those based on the one where Africa was removed (r = 0.92 and 0.93, respectively; Extended Data Figs. 7 and 9, respectively). Low correlations between the maps generated with the full dataset and those based on smaller datasets depict those regions that contributed substantially for the full model predictions (Supplementary Fig. 1), which is also correlated to the number of observations available for each continent (Supplementary Tables S2 and S4).

As predicted, our results show that wetter tropical forests tend to be more functionally diverse than drier tropical forests, especially for morphological/structural traits and foliar nutrient traits, but also more functionally redundant for foliar nutrient and photosynthetic traits than drier tropical forests (Figs. 3 and 4). While FD levels across our sampling locations are not significantly related to their taxonomic diversity (number of species, genera and families; P value > 0.05), $FRed_{NU}$ appears to be positively correlated to taxonomic diversity (P value < 0.05; Supplementary Table S5). Our results suggest that given the lower FD (Fig. 3) and FRed (Fig. 4) of drier tropical forests for most of the analysed trait groups, these forests may be more at risk in the face of further water-availability reductions.

The bivariate prediction maps combining FD and FRed (Fig. 5) highlight how wet tropical regions, such as the western Amazon, Central Africa and several regions in Southeast Asia maintain high FD and high FRed of morphological/structural (FD_{MO} max = 3.5, $FRed_{MO}$ max = 1.5) and leaf nutrient traits (FD_{NU} max = 2.5, $FRed_{NU}$ max = 1.5) and also in several wet regions for leaf photosynthetic traits (FD_{PHO} max = 2.5, $FRed_{PHO}$ max = 1.5). We expect these wet tropical regions to be more resilient to a changing climate given their

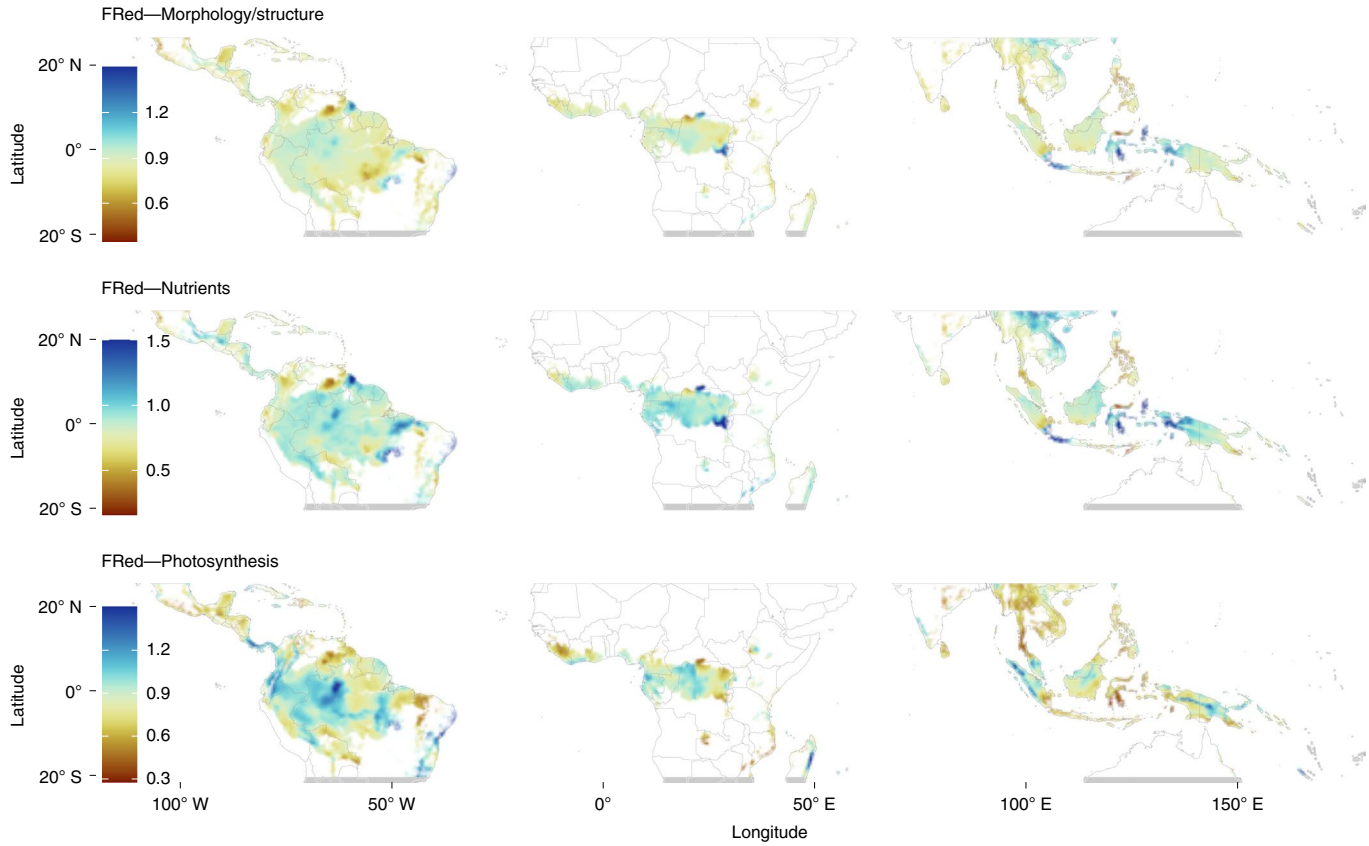

Fig. 4 | Global predictions of FRed across the tropical and subtropical dry and moist broadleaf forests. FRed predictions for morphological/structural (top panel), leaf nutrient (middle panel) and photosynthetic (bottom panel) traits are shown. Dark brown colours depict areas where FRed is lowest, light brown and light blue where FRed is intermediate and dark blue where FRed is predicted to be highest. FRed predictions across the tropics were made using the statistical models for which details are shown in Supplementary Table S3.

large combined FD (Fig. 3) and FRed (Fig. 4). To evaluate which are the different levels of FD and FRed across tropical and subtropical dry and moist broadleaf forests, we distinguished low, intermediate and high scores based on the range of the spatial predictions (Supplementary Table S6 and Methods). We predicted that only 2.4% of the tropical and subtropical dry and moist broadleaf forests have high morphological FD and 2.3% high morphological FRed. In contrast, the drier tropical forests show a FD of morphological/structural traits that reach only about half of that in the wet tropics (FD_{MO} min = ~1.5) and some of the lowest FRed (<0.6). From the total area of tropical and subtropical dry and moist broadleaf forests, 30.4% shows low morphological/structural FD and 5.5% have low morphological/structural FRed. Moreover, FD and FRed of leaf nutrient traits are lowest to intermediate across the tropical dry forest regions such as the southernmost parts of the forests in Brazil, parts of Mexico and West Africa (Figs. 3 and 4).

While 14.8% of the forest area has low foliar nutrient FD and 3.7% low FRed, 14.1% shows high nutrient FD and 7% high FRed. Drier tropical forests in western Mexico, the southern forest portion of Brazil and parts of Central Africa and West Africa show intermediate to high photosynthetic FD (max = 2.5), but they also tend to show intermediate to low levels of FRed ($FRed_{PHO}$ min = 0.3). However, photosynthesis FD and FRed do not seem to have a clear difference between wetter and drier forests. About 36.8% of the tropical and subtropical dry and moist broadleaf forest area is predicted to have low photosynthetic FD and 16.9% to have low photosynthetic FRed, while only 2.4% is expected to have high photosynthetic FD and 6.8% high photosynthetic FRed. Overall, a large amount of forest area has intermediate photosynthetic FD and/or FRed levels (60.7% and 76.3%, respectively). The bivariate FD–FRed predictions show that most tropical forests across the western Amazon and Central Africa reach some of the highest-predicted morphological and photosynthesis FD and FRed, while a smaller area of western South America reaches some of the highest-predicted nutrient FD and FRed (Fig. 5). In general, forests in drier areas show lower FD and FRed combined scores (grey colour in Fig. 5 bottom panel) for the three functional groups (morphology/structure, nutrients and photosynthesis), but this is more evident for the photosynthesis traits (Fig. 5).

Linking FD, FRed and resilience. We tested to what extent the long-term FD and FRed model predictions (Figs. 3 and 4), could capture the functioning of tropical forests after climatic disturbances such as El Niño events. By obtaining the aboveground biomass data (AGB) from a set of 86 vegetation plots in tropical Africa before and after the 2015 El Niño event[37], we calculated the change in aboveground biomass (ΔAGB) and modelled it as a function of the predicted long-term FD and FRed map scores. Bennett et al. did not detect a strong decline in AGB for most forests they analysed after the 2015 El Niño event[37]. We show that, on average, smaller decreases or larger increases in AGB (Fig. 6 and Supplementary Table S7) can be found at locations that are predicted to have higher long-term FD and FRed of morphology/structure (slope = 1.97, [0.28, 3.65]; Fig. 6a) and nutrient traits (slope = 2.94, [0.25, 5.69]; Fig. 6b) and also higher FRed of photosynthesis traits (slope = 2.96, [0.94, 5.13]; Fig. 6d) (Supplementary Table S9). The effect of FD_{NU} on ΔAGB was mediated by recent changes in MCWD (ΔMCWD), with positive FD_{NU} effects found in areas that experienced larger

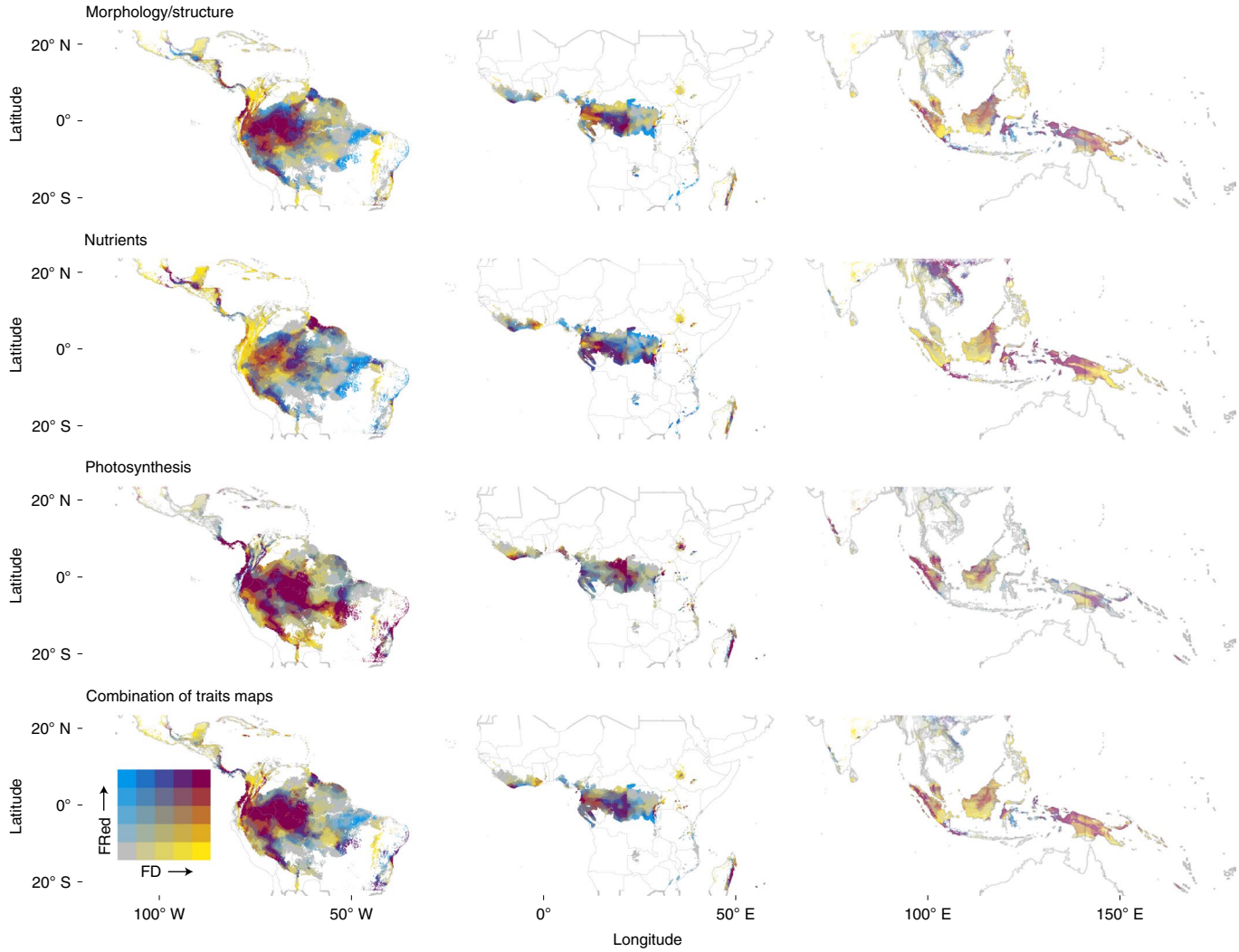

Fig. 5 | Global bivariate maps combining the scores of the FD and FRed across the tropical and subtropical dry and moist broadleaf forests. Bivariate maps for morphological/structural (top panel), leaf nutrient (second panel) and photosynthetic (third panel) traits are shown. The bottom panel shows the combination of the morphological/structural, nutrient and photosynthesis bivariate maps after standardizing (with values 0 to 1) and summing them to obtain a general bivariate map of global FD and FRed. Purple-red colours depict areas where both FD and FRed are highest, while yellow points to areas with higher FD and blue to areas with higher FRed. Grey colours show areas where both FD and FRed are predicted to be lowest. Full details of the statistical models underlying these predictions are provided in Supplementary Table S3.

increases in mean MCWD (Fig. 6b). There was no strong effect of FD_{PHO} in areas where ΔVPD was smaller (blue fitted line in Fig. 6c), but the effect became negative for areas where ΔVPD was larger (becoming drier, red fitted line in Fig. 6c). The effect of $FRed_{NU}$ on ΔAGB was mediated by ΔMCWD with a positive effect only in regions that experienced increases in water availability (Fig. 6e blue fitted line; slope = 2.94 [0.25, 5.69]).

Discussion

Changes in forest cover affect the local surface temperature by means of the exchanges of water and energy[38]. At the same time, climate change is altering land conditions, affecting the regional climate, and in the near future, global warming is likely to cause the emergence of unprecedented climatic conditions in tropical regions[38]. Therefore, determining the distribution of more and less resilient tropical forests (for example, regarding the maintenance of their functioning) to a changing climate and understanding the mechanisms causing such changes in resilience is pivotal for the conservation of biodiversity and ecosystem functioning. Here we provide spatially explicit models of forest FD and FRed that may aid on this endeavour. However, such predictions may not directly reflect the actual resilience of forest towards climate change as other biological (for example, competition, dispersal) and climatic (for example, groundwater depth, microclimate) may also play a pivotal role on the responses of tropical forests to a changing environment.

The theory on niche complementarity predicts that more diverse systems make more efficient use of ecosystem properties given the complementarity of species in the use of resources available[39,40]. High functional complementarity and FRed may be more easily achieved in areas with high taxonomic richness. Such complementarity may also increase the performance of diverse communities in the face of more stressful environments given facilitative interaction among species[41]. It therefore can be expected that more functionally diverse and more functionally redundant communities would experience lower changes in performance (for example, lower mortality, lower biomass decrease) with changes in environmental conditions (for example, ΔMCWD, ΔVPD). In our study we observed that the FD levels are not significantly related to the taxonomic diversity found in the study sites across the tropics but that FRed tends to be, especially for redundancy in morphological/structure and foliar nutrient

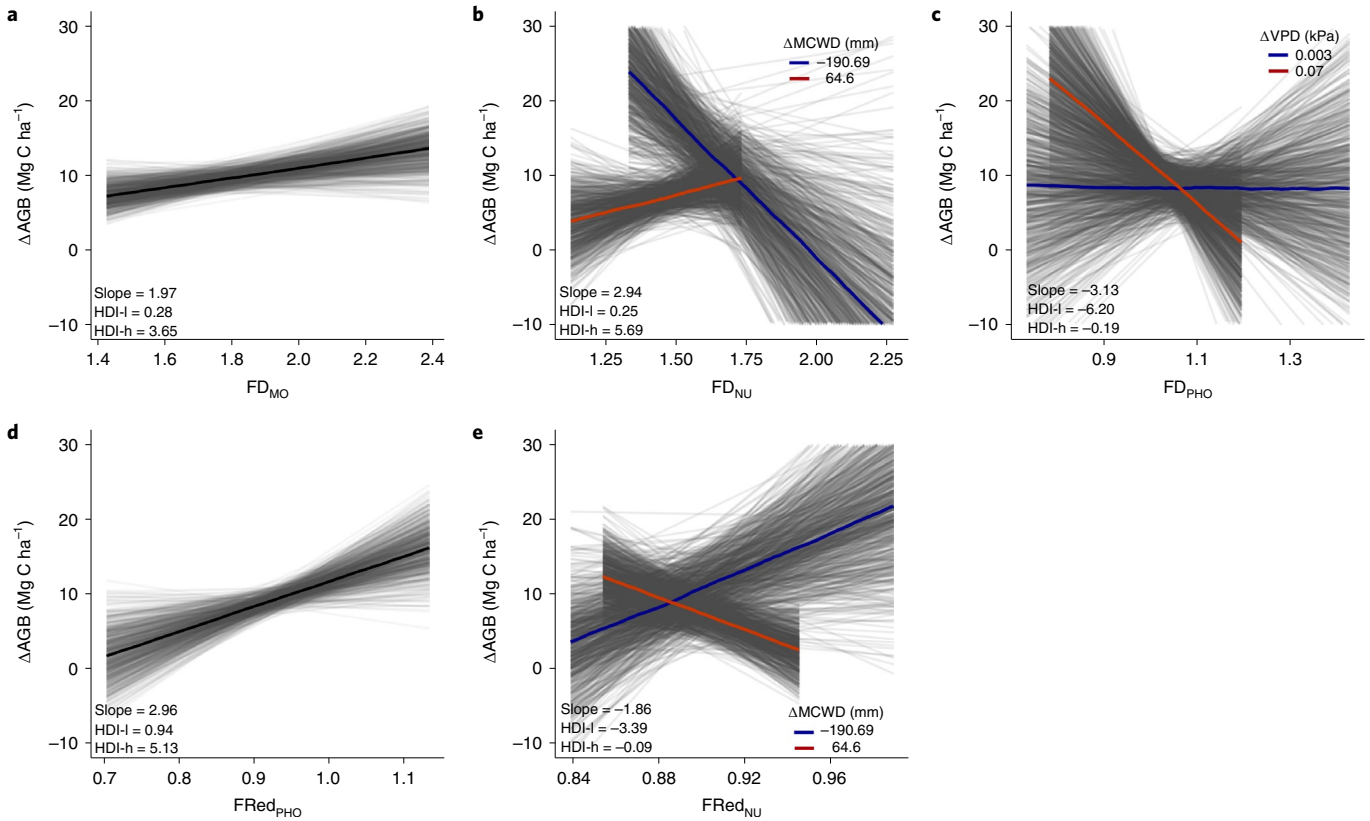

Fig. 6 | The strength of ΔAGB after the extreme 2015 El Niño event in Africa is related to the local FD and FRed. a–e, The relation between ΔAGB and FD is shown in **a–c** and between ΔAGB and FRed in **d–e**. The *x* axis shows the FD or FRed scores for the morphological/structural (MO), nutrient (NU) and photosynthetic (PHO) traits as extracted from the predictions shown in Figs. 3 and 4, and the *y* axis shows the relation with ΔAGB. The ΔAGB shows a clear relation (90% HDI does not overlap 0) with the diversity indices (Supplementary Table S7). Thick black lines show the average response, and grey shaded lines show 700 random draws from the posterior distribution representing variability of the expected model fit. The blue fitted line in **b** shows the effect of FD_{NU} at the largest decrease in ΔMCWD and the red fitted line at the larger increase in ΔMCWD. The blue fitted line in **c** shows the effect of FD_{PHO} at the largest decrease in ΔVPD and the red fitted line at the larger increase in ΔVPD. In **e**, the effect of $FRed_{NU}$ is shown for the largest decrease in ΔMCWD with the blue fitted line, and the red fitted line shows the effect at the largest increase in ΔMCWD. In **b**,**c**,**e** the thick blue and red fitted lines represent the slopes of the interaction between the variable in the *x* axis and the moderator (that is, ΔMCWD or ΔVPD). The FD and FRed scores for each trait group (that is, morphology/structure, nutrients and photosynthetic) are predictions extracted from Figs. 3 and 4 for the vegetation plots where the ΔAGB was collected. Only model covariates with a clear relationship with the ΔAGB are shown. Supplementary Table S7 provides full statistical results. ΔAGB data from Bennett et al.[37] (Supplementary Table S5).

traits. This points to the role of taxonomic diversity on the possible resilience of tropical ecosystems. We show that forest communities located in areas with lower soil and atmospheric water stress are generally more functionally diverse and more functionally redundant in morphological/structural, nutrient and photosynthetic traits than communities in drier areas. Such higher FD and higher FRed may be one reason why such forests have experienced weaker compositional and ecosystem functioning changes (for example, carbon capture) as a result of a drying climate in comparison to forests in drier areas, as shown for forests across water-availability gradients in West Africa[32,33] and the Amazon[20,25]. The higher FD in these wetter forests can be the result of their high water availability (low MCWD and VPD, Supplementary Table S2) (refs. [42,43]). These conditions facilitate the adaptation by means of a varied species morphology and structure[44] to a diverse set of light and moisture conditions under and at the canopy. Overall, our results support our expectation of lower FD in the sites with lower long-term water availability and are in agreement with what has been recently found not only for FD but also for taxonomic and phylogenetic diversity in some local forests[32,45]. Higher diversity and higher redundancy in functional traits may enhance ecosystem functioning, such as the ability of plant communities to capture carbon[46,47], and thus shows smaller reductions in biomass and lower mortality[48] under changes in climatic conditions. Our results are consistent with recent studies carried out in temperate forests[47] and with few tree taxa[26], which suggest a positive FD–productivity relationship.

Tropical forests that experienced the largest decreases in soil water availability across the past half century, which corresponds to intermediate to high long-term average MCWD (for example, some forests in Panama, Peru and southern Mexico), tend to have high morphology/structure and nutrient FD and FRed and high photosynthetic FD. The high FD and high FRed potentially point to the capabilities of such forests to better withstand the effects of a drying environment than other locations with low FD and FRed levels. Our findings show that atmospheric water availability (VPD) and its changes in the past decades mediate the FD and FRed levels across tropical forest ecosystems. Forests that experienced larger decreases in VPD over the past half century tend to be functionally redundant in morphological and nutrient traits even with increases in soil water availability (here the MCWD). However, such forests are not necessarily redundant in photosynthesis traits. One explanation for this pattern of higher redundancy of forests that

experienced larger increases in MCWD and VPD is that such increases in water stress occurred in a variety of forests that are located all across the long-term mean MCWD and VPD spectrum (Supplementary Table S2). That means that these forests may well be composed of species with a wide range of functional adaptations to local conditions, adaptations that could have a possible mechanistic link via leaf phenology[49]; some adapted to long periods of droughts but also others adapted to high water availability across the year. As tropical forests that increased the most in soil and atmospheric water availability are located across the long-term water-availability gradient, these forests might be composed of species that have evolved with different leaf strategies ranging from evergreen to sclerophyllous and deciduous[21]. Leaf adaptations to different environments may thus also explain the pattern of increasing diversity and redundancy of leaf nutrients and photosynthesis traits in these forests that experienced larger decreases in water availability. An important further step in future analyses will be to include as much information as possible not only on the changes in climate but also on the contemporary changes in FD and FRed. This would allow establishing a more direct link between the effects of a changing climate on forest functioning. Moreover, while our study showed clear relations with proxies of water availability at a pan-tropical scale (MCWD and VPD), other environmental variables at fine scale, including local topography and groundwater availability, may also contribute to determining local FD and FRed levels.

Forests with larger FD and larger FRed pools may be more resilient to further climate change. Extreme El Niño events bring about higher temperatures and droughts across tropical forests, which can impact the establishment, survival and persistence of tropical forest vegetation, thus also impacting their functioning[37]. The 2015–2016 El Niño event did not seem to strongly reduce carbon gains in African tropical forests. Although we did not measure the functional composition of those tropical forests in Africa before and after the El Niño event, our modelling framework provides a general understanding of the FD and FRed of such forests given long-term climate conditions. Our results show that areas with higher long-term FD and FRed tended to show smaller decreases or larger increases in AGB, thus being more resilient to changes in environmental conditions caused by the 2015–2016 El Niño event. Overall, our results highlight that tropical dry forests, such as those in the drier parts of Mexico, Colombia, southeastern Amazonia and much of West Africa, which have experienced high long-term soil water and atmospheric water stress over the past half century, could be at higher risk than wetter forests of further functional declines given the projected changes in climatic conditions for the coming decades[50]. Further droughts may increase the water stress of drier tropical forests, which may already be at their climatic physiological limits, and could potentially drive them towards alternative stable states[19]. This is in agreement with recent findings for West African[32] and South American drier tropical forests[6,49], where large and consistent changes in FD[20] and functioning[6] have been observed. It has been hypothesized that low FD and low FRed may pinpoint areas that could be less resilient to further changes in environmental conditions[51]. Recent work in the wet tropics of Australia shows that tree growth has been reduced the most by positive anomalies in atmospheric water deficits in drier forests and for species growing faster in drier conditions than in wetter ones[35]. The net carbon sink of tropical seasonal forests in Brazil has decreased by 0.13 Mg C ha^{-1} per year, amounting to carbon losses of 3.4% per year (on average over a 15 year period)[6], highlighting how the driest and warmest sites are experiencing some of the largest carbon-sink declines and becoming carbon sources. Moreover, the effects of a changing climate on drier tropical forest ecosystems may not only affect tree growth and survival but also strongly decrease their functional trait space available, possibly also affecting their functioning[49]. Both the species-level and forest-level differential demographic sensitivities to a drying climate support this hypothesis of potentially less resilience in already-drier environments.

We also highlight the need for measuring more widely other plant functional traits that have a more direct link to the availability, accessibility and transport of water resources and to adaptations to a drying climate such as plant hydraulic traits (for example, vessel density, vulnerability to xylem embolism (P_{50}), hydraulic safety margin, hydraulic conductivity, osmotic potential, root size and depth), which are seldom available for most tropical plant species but that may shed more light into the possible responses of a tropical forest to a changing climate[52,53]. However, recent work has shown there is strong correlation between plant hydraulics and economic traits. For instance, wood density may serve as a proxy for hydraulic traits[54] and has been shown to correlate with vessel diameter, branch and tree leaf-specific conductivity[55–57], resistance to embolism[56,58], sapwood capacitance[59,60], minimum leaf water potential[61] and leaf water potential at turgor loss[59]. Also, significant relationships between SLA and conduit diameter, seasonal change in pre-dawn leaf water potential and stomatal conductance have been found[61], together with significant correlation between leaf P_{50} and leaf mass per area (LMA) and leaf hydraulic conductivity and LMA[62]. Moreover, the leaf osmotic potential at full turgor and leaf nitrogen content have been shown to be largely correlated[63]. Given that within the hydraulic traits—and thus their leaf and wood economics correlates—and in the face of a changing environment, there is a trade-off involving drought avoidance and hydraulic safety. Such a trade-off forms an important axis of variation across tropical forests where it is expected that fast-growing species have lower hydraulic safety compared with slow-growing species[53]. Across the tropics, species that can quickly transport water resources would tend to be the ones with low wood density, short leaf life span and high rates of resources acquisition[52]. We expect this relationship to scale up from the individual to the ecosystem level and that this is thus reflected in ecosystem characteristics such as AGB.

In summary, this study addresses the need to understand and monitor the responses of tropical forest ecosystems to climate change such as the negative impacts of a drying climate on the capacity of tropical forests to sequester and store carbon. Current models of ecosystem contribution to climate mitigation lack information on earth systems feedbacks. Our results show how contemporary climate shapes the FD and FRed of tropical forest communities. Across the tropics, a diverse set of environmental conditions support a myriad of tropical tree communities with diverse combinations of plant functional traits and different FD and FRed levels. Tropical communities more at risk of shifting towards alternative states could be expected to be currently the ones where lower FD and FRed is found and that are under already high water stress, such as in the drier tropical forests. From the ecosystems conservation point of view, it is of critical importance to inform decisions by mapping tropical regions in terms of their resilience to future changes in the environment. Conservation efforts need to prioritize and manage ecosystems accordingly, especially including drier tropical forests in the conservation agenda but also considering that wet tropical forests with higher FD and higher FRed are likely to continue to be long-term carbon stores and more resilient in the face of climate extremes and pathogens.

Methods

Vegetation plots. We collected vegetation census data from 74 permanent vegetation plots that are part of the Global Ecosystems Monitoring network (GEM; http://gem.tropicalforests.ox.ac.uk)[64]. These plots are located in wet tropical forests, seasonally dry tropical forests and tropical forest–savanna transitional vegetation. The sampled vegetation plots ranged in area from 0.1 ha to 1 ha, with most (67%) being 1 ha and only one of them being 0.1 ha (Supplementary Table S2). The plots are located in Australia, Brazil, Colombia, Gabon, Ghana, Malaysian Borneo, Mexico and Peru across the four tropical continents (Supplementary Table S2). In each plot, all woody plant individuals with a diameter ≥10 cm at breast height or

above buttress roots were measured. In the plots NXV-01 and NXV-10 in Nova Xavantina, referred to hereafter as Brazil-NX, the diameter was measured at 30 cm from the ground level as is standard in drier shorter vegetation monitoring protocols.

Plant functional traits. We directly collected plant functional trait measurements from the most abundant species that would cover at least 70% of plot basal area and that were located in most of the 74 vegetation plots mentioned above (Extended Data Fig. 1 and Supplementary Table S1). All traits were collected following the GEM network standardized methodology across plots. Forest inventory data were used to stratify tree species by basal area dominance. The tree species that contributed most to basal area abundance were sampled with 3–5 replicate individuals per species. Eighty percent or more of basal area was often achieved in low diversity sites (for example, montane or dry forests). For each selected tree, a sun and a shade branch were sampled and in each branch, 3–5 leaves were used for trait measurements. This represented a total sample of 2,461 individual trees across the tropics (Extended Data Fig. 1). We collected plant functional traits related to photosynthetic capacity: A_{max} ($\mu mol\,m^{-2}\,s^{-1}$), light-saturated maximum rates of net photosynthesis at saturated CO_2 (2,000 ppm CO_2); A_{sat} ($\mu mol\,m^{-2}\,s^{-1}$), light-saturated rates of net photosynthesis at ambient CO_2 concentration (400 ppm CO_2); and R_{Dark} ($\mu mol\,m^{-2}\,s^{-1}$), dark respiration. We also collected leaf nutrient concentration traits (%) of Ca, leaf calcium; K, leaf potassium; Mg, leaf magnesium; N, leaf nitrogen; and P, leaf phosphorus. We measured plant morphological and structural traits: A (cm^2), leaf area; DM (g), leaf dry mass; FM (g), leaf fresh mass; LDMC ($mg\,g^{-1}$), leaf dry matter content; LWC (%), leaf water content; SLA ($g\,m^{-2}$); T (mm), leaf thickness; and WD ($g\,cm^{-3}$), wood density. Further details of measurements for the Peruvian Andes campaign are given in Martin et al.[65] and Enquist et al.[66], for the Malaysian campaign in Both et al.[67] and for the Ghana and Brazil campaigns in Oliveras et al.[68] and Gvozdevaite et al.[69] and for the Colombia campaigns in González-M et al.[49]. For the specific dates of collection of plant functional traits, see ref. [70]. For the FD and FRed calculations, as both only accept one trait value per species, from the individual-level plant functional traits, we averaged the values at the species level and when the species had no trait values available, we filled the gaps by averaging the trait values at the genus level. This protocol allowed us to have at least 70% of the plot's basal area covered by traits but often more. Thus, in our analysis the inclusion of plots is trait dependent in the sense that only plots with at least 70% of the basal area covered by the focus trait were included in the analysis (Supplementary Table S2).

Community-level FD and FRed. We calculated the FD and FRed of morphological/structural traits, leaf chemistry and photosynthetic traits, which are hypothesized to be of importance for tropical forests to respond to a drying climate (Supplementary Table S1) (refs. [14,21]), based on data for species covering at least 70% of the plot basal area (Supplementary Table S2) and following equations from refs. [34,71–73]. The morphological/structural and nutrient-related traits used for this analysis are A, FM, DM, LDMC, T, LWC, SLA, WD, Ca, K, Mg, N and P, and A_{sat}, A_{max} and R_{Dark} for photosynthesis. We did not build an index including all functional traits together as this would make their interpretation rather difficult as they point to different axes of the global spectrum of plant form and function[74] and also because of the difference in number of records available for each trait group. Plant FD was calculated at the plot level using the functional dispersion metric, which is closely related to the Rao quadratic diversity index Q and which represents the mean distance, in trait space, of each single species to the weighted centroid of all species[34]. We used the FD as it can handle any number and type of traits, and because it is unaffected by species richness, it weighs the values based on the abundance of species and is not influenced by outliers and is relatively insensitive to the effects of undersampling[75]. To calculate FD we applied the equation presented by Laliberté and Legendre[34]:

$$\mathrm{FD} = \frac{\sum \mathrm{BA}_{ip}\, z_{ip}}{\sum \mathrm{BA}_{ip}} \quad (1)$$

where BA_{ip} reflects the total plot-level basal area of species i in plot p, and z_{ip} is the distance of species i in plot p to the weighted centroid of the n species in trait space. The plant traits were weighted by the relative basal area (in m^2) of each of the species in the plot. Therefore, FD summarizes the trait diversity and represents the mean distance in trait space of each species to the centroid of all species in a given community. All numeric traits were standardized during the FD calculation.

We calculated the functional trait redundancy in the community (vegetation plots), FRed, as in Pavoine and Ricotta[72] and Ricotta et al. ('Rstar')[73] and as developed in the 'uniqueness' function of the R 'adiv' package[71]. 'Rstar' quantifies how redundant a plant community is compared with a scenario where all species would have the most distinct trait values possible. As in the case of FD, 'Rstar' as calculated in Ricotta et al.[71,72] works with multiple traits and takes into account species abundances. The 'Rstar' index is complementary to the community-level functional uniqueness index Ustar described by Ricotta et al.[72], which is the ratio of the Rao quadratic diversity index Q[76,77] that accounts for species trait dissimilarities and the Simpson index D, which considers the species in the community as equally and maximally dissimilar. Thus Ustar measures the uniqueness of the community in functional space, which is obtained by including interspecies dissimilarities in the calculations of the index. Rstar, which is the complement of Ustar, represents thus a measure of community-level FRed and is quantified as:

$$\mathrm{Ustar} = \frac{1 - D}{1 - Q} \quad (2)$$

$$\mathrm{Rstar} = 1 - \mathrm{Ustar} \quad (3)$$

For an in-depth description of the FRed index, see refs. [71–73].

All above-mentioned analyses were carried out in the R statistical environment[78] with the 'FD' and 'adiv' packages.

Climatic and soil data. To investigate the role that long-term climate plays on determining the community trait composition and FD and FRed across tropical forests, we gathered climatic data on the potential evapotranspiration (PET in mm), precipitation accumulation (mm) and VPD (kPa) from the TerraClimate project[79] at a spatial resolution of ~4 × 4 km. The data were obtained for the period from 1958 to 2017. Using the full-term climatic dataset (1958–2017), we calculated the mean annual VPD, PET, precipitation coefficient of variation (CV, as a measure of seasonality in water availability) and the MCWD. The MCWD is a metric for drought intensity and severity and is defined as the most negative value of the climatological water deficit (CWD) over each calendar year. The VPD is an indicator of plant transpiration and water loss[14]. CWD is defined as precipitation (P) (mm per month) − PET (mm per month) with a minimum deficit of 0. The MCWD was calculated as in Malhi et al.[13], where MCWD = min (CWD1… CWD12). As a final step, we converted the MCWD so that positive values indicate increases in water stress. We also calculated the change in the climatic variables (ΔMCWD, ΔVPD and ΔCV) between a first period corresponding to a climatology of 30 years encompassing 1958–1987 and a second period encompassing the years 1988–2017. The climatology of 30 years to calculate the different time periods' climate was selected as recommended by the World Meteorological Organization to characterize the average weather conditions for a given area (https://public.wmo.int/en/about-us/frequently-asked-questions/climate). There are other possibly relevant predictors of water stress for plants in tropical forests such as the water table depth[17,80]. It has been hypothesized that the water table depth drives the distribution of plant species and functional composition, and where it is expected that forests in shallow water table areas show higher mortality during strong drought events (for example, El Niño) given the presence of species with shallower roots and less adapted traits[17,80]. However, we did not include the water table depth in our analysis given the lack of spatially explicit predictions across the tropics.

We also obtained soil texture (percent of clay and sand) and chemistry (soil pH and CEC) gridded data from the SoilGrids project (https://soilgrids.org/) and used this as extra covariates in our modelling framework. Although the CEC includes the acid aluminium, which is not a plant nutrient and may be toxic to plants, this is one of the best estimates of the overall potential of the soil to exchange cations (Ca, Mg and K) that is available at a pantropical extent[81].

We then tested the correlation between all pairs of climatic variables (full-term and their changes) and also between the soil variables. We observed that MCWD and CV had Pearson's correlation coefficients |>0.70| and also CEC and pH and clay and sand had correlation coefficients |>0.70| (Supplementary Fig. 2), and we thus dropped CV and its change, sand and pH from the analyses to avoid distorting model coefficients in the modelling stage[82]. We then carried out a PCA using the MCWD and VPD climatic variables (average of full-term and their changes) and another with the soil variables to investigate the distribution of the vegetation plots in the climate and soil space and to describe how much of this distribution can be explained by each of these. For the PCA analysis, we used the 'stats' package in R.

Statistical analysis. *FD and FRed statistical analysis.* We investigated the variation in morphological/structural, leaf chemistry and photosynthetic FD and FRed across tropical forests by modelling their relation with mean MCWD, VPD for the period 1958–2017 and their interaction, the ΔMCWD and ΔVPD between the first and second periods and their interaction and soil chemistry (CEC) and texture (clay %). For the photosynthesis statistical models, given their lower sample size (n = 22; Supplementary Table S2), interaction terms were not included, and to avoid overfitting, we first tested by means of leave-one-out cross-validation[83] if the soil covariates improved or not the models with only climate information. We found soil data did not improve our models (Supplementary Table S8) and thus left CEC and clay out of the photosynthesis models. We also calculated the relative change (%) in climatic conditions, but this did not improve model predictions and thus we present only results that include the absolute changes in MCWD and VPD. We included the change in MCWD and VPD as we wanted to understand if areas that have experienced stronger changes in climate showed lower or higher FD and FRed than others that have experienced milder climate changes. In the same way, we included the interaction between MCWD and VPD (and also between ΔMCWD and ΔVPD) as there may be regions where high values of one of these variables may not be related to the values of the other; for example high MCWD may not be related to high VPD. Before the statistical modelling, we centred and standardized (generated z-scores) all climatic and soil variables.

We tested for spatial autocorrelation effects in the FD and FRed model residuals using the Moran's *I* test and found a significant effect for the photosynthesis and nutrients FD models and for the FRed nutrients model (Supplementary Table S9). Thus, for those data, we calculated the spatial distance at which such spatial effect decreased and found that a distance of 2 km was sufficient. We then generated an identification (ID) for each group of plots (group ID) that were, at most, 2 km away from each other and included such group ID as a random factor in those statistical models. As some plots were smaller than 1 ha (Supplementary Table S2), we included the *z*-scores of plot size as a covariate in all statistical models to account for its possible effect. We log transformed the FD and FRed indices to improve the normality of the data and applied linear mixed-effects models with a Gaussian error structure accounting for difference in plot size and spatial autocorrelation as described above under a Bayesian framework. The mixed-effects models were run with normal diffuse priors with mean 0 and 2.5 standard deviation to adjust the scale of coefficients and 10 standard deviations to adjust the scale of the intercept, three chains and 10,000 iterations to avoid issues with model convergence. We computed the HDI, rendering the range containing the 90% most probable effect values, and calculated the region of practical equivalence values using such HDI as suggested in Makowski et al.[84]. The 95% HDI was not used as this range has been shown to be unstable with effective sample size <10,000 (ref. [85]). We considered that a climatic variable had an important (significant) effect on the response variable if the 90% HDI did not overlap 0. Posterior density distributions for all models and covariates included in the models are shown in Supplementary Fig. 3 and Supplementary Fig. 4.

On the basis of the statistical models described above, we created spatial predictions of FD and FRed at a pantropical scale. We defined the 'low', 'intermediate' and 'high' FD and FRed groups by defining the range in FD and FRed values and dividing that range between three to allocate the FD and FRed predicted values to each of these groups and to state what is the predicted percent area of tropical and subtropical dry and moist broadleaf forests with low, medium and high FD and FRed. We also tested the robustness of the spatial predictions of FD and FRed by developing the models by leaving out the data from one continent (Southeast Asia and Australia together), fitting the model again and comparing the resulting spatial predictions to the full model prediction maps by means of Spearman correlations. In Extended Data Fig. 10, we also highlight locations across the tropics with climate and soil conditions outside of our climatic and soil calibration space thus not covered by the range in our sampling locations, which may represent locations where our models are extrapolating the relationships found.

Relating FD, FRed and biomass. We obtained the AGB data from an independent set of 100 vegetation plots in Africa before (AGB_{pre}) and after (AGB_{post}) the 2015 El Niño event from Bennett et al.[37]. The plots from Bennet et al. include censuses from 2000 onward where the median plot size is 1 ha, the mean initial census was May 2008, the mean pre-El Niño census was in April 2014 and the mean post-El Niño census in February 2017. The plots have a mean monitoring length pre-El Niño of 8.3 years, with a mean length of the El Niño interval being 2.7 years. To calculate AGB, Bennet et al.[37] used the 'BiomasaFP' R package, including the calculation of the census interval corrections for AGB where pre-El Niño means of these variables are time weighted using the census interval lengths. For a full description of the AGB data, see Bennett et al.[37]. We calculated the ΔAGB as:

$$\Delta\mathrm{AGB} = \left(\mathrm{AGB}_{\mathrm{post}} - \mathrm{AGB}_{\mathrm{pre}}\right) \quad (4)$$

Before modelling, we eliminated statistical outliers in the AGB values, that is, values more than 1.5 the interquartile range above the third quartile or below the first quartile. We therefore used only 86 plots in our analysis. We modelled the ΔAGB as a function of the predicted (above) FD and FRed maps scores from each functional group (morphology/structure, nutrients and photosynthesis; Figs. 3 and 4); one model was built per functional group. Each model included the FD and FRed index (for example, FD and FRed of nutrients) and their interaction with ΔMCWD and ΔVPD as to test the effect of a changing climate on the effects of FD and FRed on ΔAGB. We accounted for plot size by including it as a covariate in the models and used a Gaussian error structure model under a Bayesian framework. The ΔAGB statistical models were run with normal diffuse priors with three chains and 5,000 iterations.

We carried out all statistical analyses in the R statistical environment[78] using the, 'rstanarm', 'loo', 'bayestestR', 'egg' and 'BEST' packages.

Reporting Summary. Further information on research design is available in the Nature Research Reporting Summary linked to this article.

Data availability

The vegetation census and plant functional traits data that support the findings of this study are available from their sources (www.ForestPlots.net and gem.tropicalforests.ox.ac.uk/). To comply with the original data owners, the processed community-level data used in this study can be accessed through the corresponding author upon request.

Code availability

All relevant R functions and code used in this study are referred to in the Methods section and can be accessed at https://doi.org/10.5281/zenodo.6367982.

Received: 2 September 2021; Accepted: 24 March 2022;
Published online: 16 May 2022

References

1. Barlow, J. et al. Anthropogenic disturbance in tropical forests can double biodiversity loss from deforestation. *Nature* **535**, 144–147 (2016).
2. Beech, E., Rivers, M., Oldfield, S. & Smith, P. P. GlobalTreeSearch: the first complete global database of tree species and country distributions. *J. Sustain.* **36**, 454–489 (2017).
3. ter Steege, H. et al. The discovery of the Amazonian tree flora with an updated checklist of all known tree taxa. *Sci. Rep.* **6**, 29549 (2016).
4. Hubau, W. et al. Asynchronous carbon sink saturation in African and Amazonian tropical forests. *Nature* **579**, 80–87 (2020).
5. Pan, Y. et al. A large and persistent carbon sink in the world's forests. *Science* **333**, 988–993 (2011).
6. Maia, V. A. et al. The carbon sink of tropical seasonal forests in southeastern Brazil can be under threat. *Sci. Adv.* **6**, eabd4548 (2020).
7. Malhi, Y. et al. The regional variation of aboveground live biomass in old-growth Amazonian forests. *Glob. Change Biol.* **12**, 1107–1138 (2006).
8. Phillips, O. L. et al. Drought sensitivity of the Amazon rainforest. *Science* **323**, 1344–1347 (2009).
9. Malhi, Y. et al. Climate change, deforestation, and the fate of the Amazon. *Science* **319**, 169–172 (2008).
10. Gatti, L. V. et al. Amazonia as a carbon source linked to deforestation and climate change. *Nature* **595**, 388–393 (2021).
11. Hisano, M., Searle, E. B. & Chen, H. Y. Biodiversity as a solution to mitigate climate change impacts on the functioning of forest ecosystems. *Biol. Rev.* **93**, 439–456 (2018).
12. Pecl, G. T. et al. Biodiversity redistribution under climate change: impacts on ecosystems and human well-being. *Science* **355**, eaai9214 (2017).
13. Malhi, Y. et al. Exploring the likelihood and mechanism of a climate-change-induced dieback of the Amazon rainforest. *Proc. Natl Acad. Sci. USA* **106**, 20610–20615 (2009).
14. Seager, R. et al. Climatology, variability, and trends in the US vapor pressure deficit, an important fire-related meteorological quantity. *J. Appl. Meteorol. Climatol.* **54**, 1121–1141 (2015).
15. Smith, M. N. et al. Empirical evidence for resilience of tropical forest photosynthesis in a warmer world. *Nat. Plants* **6**, 1225–1230 (2020).
16. Yuan, W. et al. Increased atmospheric vapor pressure deficit reduces global vegetation growth. *Sci. Adv.* **5**, eaax1396 (2019).
17. Costa, F. R. C., Schietti, J., Stark, S. C. & Smith, M. N. The other side of tropical forest drought: do shallow water table regions of Amazonia act as large-scale hydrological refugia from drought?. *New Phytol.* https://doi.org/10.1111/nph.17914 (2022).
18. Brodribb, T. J., Powers, J., Cochard, H. & Choat, B. Hanging by a thread? Forests and drought. *Science* **368**, 261–266 (2020).
19. Allen, K. et al. Will seasonally dry tropical forests be sensitive or resistant to future changes in rainfall regimes? *Environ. Res. Lett.* **12**, 023001 (2017).
20. Esquivel-Muelbert, A. et al. Compositional response of Amazon forests to climate change. *Glob. Change Biol.* **25**, 39–56 (2019).
21. Aguirre-Gutiérrez, J. et al. Drier tropical forests are susceptible to functional changes in response to a long-term drought. *Ecol. Lett.* **22**, 855–865 (2019).
22. Cadotte, M. W., Carscadden, K. & Mirotchnick, N. Beyond species: functional diversity and the maintenance of ecological processes and services. *J. Appl. Ecol.* **48.5**, 1079–1087 (2011).
23. Aguirre-Gutiérrez, J. et al. Butterflies show different functional and species diversity in relationship to vegetation structure and land use. *Glob. Ecol. Biogeogr.* **26**, 1126–1137 (2017).
24. Arruda Almeida, B. et al. Comparing species richness, functional diversity and functional composition of waterbird communities along environmental gradients in the neotropics. *PLoS ONE* **13**, e0200959 (2018).
25. Yachi, S. & Loreau, M. Biodiversity and ecosystem productivity in a fluctuating environment: the insurance hypothesis. *Proc. Natl Acad. Sci. USA* **96**, 1463–1468 (1999).
26. Correia, D. L. P., Raulier, F., Bouchard, M. & Filotas, É. Response diversity, functional redundancy, and post-logging productivity in northern temperate and boreal forests. *Ecol. Appl.* **28**, 1282–1291 (2018).
27. Elmqvist, T. et al. Response diversity, ecosystem change, and resilience. *Front. Ecol. Environ.* **1**, 488–494 (2003).
28. Loreau, M. & de Mazancourt, C. Biodiversity and ecosystem stability: a synthesis of underlying mechanisms. *Ecol. Lett.* **16**, 106–115 (2013).
29. Petchey, O. L., Evans, K. L., Fishburn, I. S. & Gaston, K. J. Low functional diversity and no redundancy in British avian assemblages. *J. Anim. Ecol.* **76**, 977–985 (2007).

30. Jucker, T. et al. Stabilizing effects of diversity on aboveground wood production in forest ecosystems: linking patterns and processes. *Ecol. Lett.* **17**, 1560–1569 (2014).
31. Fonseca, C. R. & Ganade, G. Species functional redundancy, random extinctions and the stability of ecosystems. *J. Ecol.* **89**, 118–125 (2001).
32. Aguirre-Gutiérrez, J. et al. Long-term droughts may drive drier tropical forests towards increased functional, taxonomic and phylogenetic homogeneity. *Nat. Commun.* **11**, 3346 (2020).
33. Fauset, S. et al. Drought-induced shifts in the floristic and functional composition of tropical forests in Ghana. *Ecol. Lett.* **15**, 1120–1129 (2012).
34. Laliberté, E. & Legendre, P. A distance-based framework for measuring functional diversity from multiple traits. *Ecology* **91**, 299–305 (2010).
35. Bauman, D. et al. Tropical tree growth sensitivity to climate is driven by species intrinsic growth rate and leaf traits. *Glob. Change Biol.* **28**, 1414–1432 (2022).
36. Quesada, C. et al. Basin-wide variations in Amazon forest structure and function are mediated by both soils and climate. *Biogeosciences* **9**, 2203–2246 (2012).
37. Bennett, A. C. et al. Resistance of African tropical forests to an extreme climate anomaly. *Proc. Natl Acad. Sci. USA* **118**, e2003169118 (2021).
38. *Climate Change and Land: An IPCC Special Report on Climate Change, Desertification, Land Degradation, Sustainable Land Management, Food Security, and Greenhouse Gas Fluxes in Terrestrial Ecosystems* (eds Shukla, P.R. et al.) (IPCC, 2019).
39. Ashton, I. W., Miller, A. E., Bowman, W. D. & Suding, K. N. Niche complementarity due to plasticity in resource use: plant partitioning of chemical N forms. *Ecology* **91**, 3252–3260 (2010).
40. Petchey, O. L. On the statistical significance of functional diversity effects. *Funct. Ecol.* **18**, 297–303 (2004).
41. Bruno, J. F., Stachowicz, J. J. & Bertness, M. D. Inclusion of facilitation into ecological theory. *Trends Ecol. Evol.* **18**, 119–125 (2003).
42. ter Steege, H. et al. Continental-scale patterns of canopy tree composition and function across Amazonia. *Nature* **443**, 444–447 (2006).
43. Raes, N. et al. Botanical richness and endemicity patterns of Borneo derived from species distribution models. *Ecography* **32**, 180–192 (2009).
44. Shenkin, A. et al. The influence of ecosystem and phylogeny on tropical tree crown size and shape. *Front. For. Glob. Change* **3**, 501757 (2020).
45. Harrison, S., Spasojevic, M. J. & Li, D. Climate and plant community diversity in space and time. *Proc. Natl Acad. Sci. USA* **117**, 4464–4470 (2020).
46. Grossman, J. J., Cavender-Bares, J., Hobbie, S. E., Reich, P. B. & Montgomery, R. A. Species richness and traits predict overyielding in stem growth in an early-successional tree diversity experiment. *Ecology* **98**, 2601–2614 (2017).
47. Williams, L. J. et al. Remote spectral detection of biodiversity effects on forest biomass. *Nat. Ecol. Evol.* **5**, 46–54 (2021).
48. Hutchison, C., Gravel, D., Guichard, F. & Potvin, C. Effect of diversity on growth, mortality, and loss of resilience to extreme climate events in a tropical planted forest experiment. *Sci. Rep.* **8**, 15443 (2018).
49. González-M, R. et al. Diverging functional strategies but high sensitivity to an extreme drought in tropical dry forests. *Ecol. Lett.* **24**, 451–463 (2021).
50. Hoegh-Guldberg, O. et al. in *IPCC Special Report on Global Warming of 1.5 °C* (eds Masson-Delmotte, V. et al.) Ch. 3 (WMO, 2018).
51. de la Riva, E. G. et al. The importance of functional diversity in the stability of Mediterranean shrubland communities after the impact of extreme climatic events. *J. Plant Ecol.* **10**, 281–293 (2017).
52. Reich, P. B. The world-wide "fast-slow" plant economics spectrum: a traits manifesto. *J. Ecol.* **102**, 275–301 (2014).
53. Oliveira, R. S. et al. Linking plant hydraulics and the fast–slow continuum to understand resilience to drought in tropical ecosystems. *New Phytol.* **230**, 904–923 (2021).
54. Anderegg, W. R. L. & Meinzer, F. C. in *Functional and Ecological Xylem Anatomy* (ed Hacke, U.) Ch. 9 (Springer, 2015).
55. Chave, J. et al. Towards a worldwide wood economics spectrum. *Ecol. Lett.* **12**, 351–366 (2009).
56. Pratt, R., Jacobsen, A., Ewers, F. & Davis, S. Relationships among xylem transport, biomechanics and storage in stems and roots of nine Rhamnaceae species of the California chaparral. *New Phytol.* **174**, 787–798 (2007).
57. Zanne, A. E. et al. Angiosperm wood structure: global patterns in vessel anatomy and their relation to wood density and potential conductivity. *Am. J. Bot.* **97**, 207–215 (2010).
58. Bucci, S. J. et al. The stem xylem of Patagonian shrubs operates far from the point of catastrophic dysfunction and is additionally protected from drought-induced embolism by leaves and roots. *Plant Cell Environ.* **36**, 2163–2174 (2013).
59. Meinzer, F. C. et al. Coordination of leaf and stem water transport properties in tropical forest trees. *Oecologia* **156**, 31–41 (2008).
60. Scholz F. G., Phillips N. G., Bucci S. J., Meinzer F. C. & Goldstein G. in *Size- and Age-Related Changes in Tree Structure and Function* (eds Meinzer F. C. C. et al.) 341–361 (Springer, 2011).
61. Mitchell, P. J. et al. Using multiple trait associations to define hydraulic functional types in plant communities of south-western Australia. *Oecologia* **158**, 385–397 (2008).
62. Villagra, Mariana et al. Functional relationships between leaf hydraulics and leaf economic traits in response to nutrient addition in subtropical tree species. *Tree Physiol.* **33**, 1308–1318 (2013).
63. Ishida, Atsushi et al. Coordination between leaf and stem traits related to leaf carbon gain and hydraulics across 32 drought-tolerant angiosperms. *Oecologia* **156**, 193–202 (2008).
64. Malhi, Y. et al. The Global Ecosystems Monitoring network: monitoring ecosystem productivity and carbon cycling across the tropics. *Biol. Conserv.* **253**, 108889 (2021).
65. Martin, R. E. et al. Covariance of sun and shade leaf traits along a tropical forest elevation gradient. *Front. Plant Sci.* **10**, 1810 (2020).
66. Enquist, B. J. et al. Assessing trait-based scaling theory in tropical forests spanning a broad temperature gradient. *Glob. Ecol. Biogeogr.* **26**, 1357–1373 (2017).
67. Both, S. et al. Logging and soil nutrients independently explain plant trait expression in tropical forests. *New Phytol.* **221**, 1853–1865 (2019).
68. Oliveras, I. et al. The influence of taxonomy and environment on leaf trait variation along tropical abiotic gradients. *Front. For. Glob. Change* https://doi.org/10.3389/ffgc.2020.00018 (2020).
69. Gvozdevaite, A. et al. Leaf-level photosynthetic capacity dynamics in relation to soil and foliar nutrients along forest–savanna boundaries in Ghana and Brazil. *Tree Physiol.* **38**, 1912–1925 (2018).
70. Aguirre-Gutiérrez, J. et al. Pantropical modelling of canopy functional traits using Sentinel-2 remote sensing data. *Remote Sens. Environ.* **252**, 112122 (2021).
71. Pavoine, S. adiv: an R package to analyse biodiversity in ecology. *Methods Ecol. Evol.* **11**, 1106–1112 (2020).
72. Pavoine, S. & Ricotta, C. A simple translation from indices of species diversity to indices of phylogenetic diversity. *Ecol. Ind.* **101**, 552–561 (2019).
73. Ricotta, C. et al. Measuring the functional redundancy of biological communities: a quantitative guide. *Methods Ecol. Evol.* **7**, 1386–1395 (2016).
74. Díaz, S. et al. The global spectrum of plant form and function. *Nature* **529**, 167–171 (2016).
75. van der Plas, F., Van Klink, R., Manning, P., Olff, H. & Fischer, M. Sensitivity of functional diversity metrics to sampling intensity. *Methods Ecol. Evol.* **8**, 1072–1080 (2017).
76. Rao, C. R. Diversity and dissimilarity coefficients: a unified approach. *Theor. Popul. Biol.* **21**, 24–43 (1982).
77. Simpson, E. H. Measurement of diversity. *Nature* https://doi.org/10.1038/163688a0 (1949).
78. R Core Team *R: A Language and Environment for Statistical Computing* (R Foundation for Statistical Computing, 2019).
79. Abatzoglou, J. T., Dobrowski, S. Z., Parks, S. A. & Hegewisch, K. C. TerraClimate, a high-resolution global dataset of monthly climate and climatic water balance from 1958–2015. *Sci. Data* **5**, 170191 (2018).
80. Fan, Y. Groundwater in the earth's critical zone: relevance to large-scale patterns and processes. *Water Resour. Res.* **51**, 3052–3069 (2015).
81. Moulatlet, G. M. et al. Using digital soil maps to infer edaphic affinities of plant species in Amazonia: problems and prospects. *Ecol. Evol.* **7**, 8463–8477 (2017).
82. Dormann, C. F. et al. Collinearity: a review of methods to deal with it and a simulation study evaluating their performance. *Ecography* **36**, 27–46 (2013).
83. Vehtari, A., Gelman, A. & Gabry, J. Practical Bayesian model evaluation using leave-one-out cross-validation and WAIC. *Stat. Comput.* **27**, 1413–1432 (2017).
84. Makowski, D., Ben-Shachar, M. S. & Lüdecke, D. bayestestR: Describing effects and their uncertainty, existence and significance within the Bayesian framework. *J. Open Source Softw.* **4**, 1541 (2019).
85. Kruschke, J. K. *Doing Bayesian Data Analysis: A Tutorial with R, JAGS, and Stan* (Academic Press, 2014).

Acknowledgements

This work is a product of the Global Ecosystems Monitoring (GEM) network (gem.tropicalforests.ox.ac.uk). J.A.-G. was funded by the Natural Environment Research Council (NERC; NE/T011084/1) and the Oxford University Jhon Fell Fund (10667). The traits field campaign was funded by a grant to Y.M. from the European Research Council (advanced grant GEM-TRAIT: 321131) under the European Union's Seventh Framework Programme (FP7/2007–2013) with additional support from NERC grant NE/D014174/1 and NE/J022616/1 for traits work in Peru, NERC grant ECOFOR (NE/K016385/1) for traits work in Santarem, NERC grant BALI (NE/K016369/1) for plot and traits work in Malaysia and ERC advanced grant T-FORCES (291585) to O.L.P. for traits work in Australia. Plot setup in Ghana and Gabon was funded by a NERC grant NE/I014705/1 and by the Royal Society-Leverhulme Africa Capacity Building Programme. The Malaysia campaign was also funded by NERC grant NE/K016253/1. Plot inventories in Peru were supported by funding from the US National Science Foundation Long-Term Research in Environmental Biology program (LTREB; DEB 1754647) and

the Gordon and Betty Moore Foundation Andes–Amazon Program. Plots inventories in Nova Xavantina (Brazil) were supported by the National Council for Scientific and Technological Development (CNPq), Long Term Ecological Research Program (PELD), process 441244/2016–5 and the Foundation of Research Support of Mato Grosso (FAPEMAT), Project ReFlor, process 589267/2016. During data collection, I.O.M. was supported by a Marie Curie Fellowship (FP7-PEOPLE-2012-IEF-327990). GEM trait data in Gabon were supported by the Gabon National Parks Agency. D.B. was funded by the Belgian American Educational Foundation (BAEF) and the European Union's Horizon 2020 research and innovation programme under the Marie Skłodowska-Curie grant agreement number 895799. W.D.K. acknowledges funding from the University of Amsterdam via a starting grant and through the Faculty Research Cluster 'Global Ecology'. S.A.-B. acknowledges funding from The Leverhulme Trust—Royal Society of the United Kingdom (A130026) under the Water Stress, Ecosystem Function and tree FD in tropical African forests project. C.A.J. acknowledges support from the Brazilian National Research Council/CNPq (PELD process 403710/2012–0), NERC and the State of São Paulo Research Foundation/FAPESP as part of the projects Functional Gradient, PELD/BIOTA and ECOFOR (processes 2003/12595-7, 2012/51509-8 and 2012/51872-5, within the BIOTA/FAPESP Program—The Biodiversity Virtual Institute (www.biota.org.br); COTEC/IF 002.766/2013 and 010.631/2013 permits. B.S.M. was supported by the CNPq/PELD projects (number 441244/2016-5 and number 441572/2020-0) and CAPES (number 136277/2017-0). D.F.R.P.B. thanks the financial support from NERC (NE/K016253/1) for trait data collection in Sabah Malaysia. M.S. acknowledges funding for Andes Biodiversity and Ecosystem Research Group (ABERG) plot network from the US National Science Foundation (NSF) Long-Term Research in Environmental Biology (LTREB) 1754647, the Gordon and Betty Moore Foundation's Andes to Amazon Initiative and RAINFOR. E.B, J.B. and Y.M. acknowledge the support from NERC under projects NE/K016431/1 and NE/S01084X/1. R.M.E. acknowledges support from the Sime Darby Foundation. Measurements and analysis include support from NERC ('AMAZONICA', NE/F005806; 'BIO-RED', NE/N012542/1; ARBOLES, NE/S011811/1), the Moore Foundation and the AfriTRON and RAINFOR networks. Y.M. is supported by the Jackson Foundation.

Author contributions

J.A.-G. conceived the study, designed and carried out the analysis and wrote the first draft of the paper. E.B. contributed to the main ideas and design of the study. Y.M. conceived and implemented the GEM Network, obtained funding for most of the GEM traits field campaigns and commented on earlier versions of the manuscript. J.A.-G., E.B., I.O.M., D.B., J.J.C.-R., M.G.N.-M., S.B., J.E.N., F.E.O., N.N.B., V.M., J.W.D., K.H., A.F., R.G.-M., N.N., A.B.H.-M., D.G., B.S.-N., S.M.R., M.M.M.S., W.F.-R., A.S., T.R., C.A.J.G., S.M., K.A., G.P.A., L.P.B., D.F.R.P.B., L.A.C., B.J.E., R.M.E., J.F., K.J.J., C.A.J., B.H.M.-J., R.E.M., P.S.M., O.L.P., A.C.B., S.L.L., C.A.Q., B.S.M., W.D.K., M.S., Y.A.T., L.J.T.W., N.S., D.A.C., J.B., S.A.-B. and Y.M. participated in or coordinated vegetation, trait data and/or soil data collection or processed field data and commented on and approved the manuscript.

Competing interests

The authors declare no competing interests.

Additional information

Extended data is available for this paper at https://doi.org/10.1038/s41559-022-01747-6.

Supplementary information The online version contains supplementary material available at https://doi.org/10.1038/s41559-022-01747-6.

Correspondence and requests for materials should be addressed to Jesús Aguirre-Gutiérrez.

Peer review information *Nature Ecology & Evolution* thanks Vinícius Andrade Maia, Flávia Costa, Rebecca Ostertag and the other, anonymous, reviewer(s) for their contribution to the peer review of this work. Peer reviewer reports are available.

Reprints and permissions information is available at www.nature.com/reprints.

Publisher's note Springer Nature remains neutral with regard to jurisdictional claims in published maps and institutional affiliations.

[1]Environmental Change Institute, School of Geography and the Environment, University of Oxford, Oxford, UK. [2]Biodiversity Dynamics, Naturalis Biodiversity Center, Leiden, the Netherlands. [3]Lancaster Environment Centre, Lancaster University, Lancaster, UK. [4]AMAP (Botanique et Modélisation de l'Architecture des Plantes et des Végétations), Université de Montpellier, CIRAD, CNRS, INRAE, IRD, Montpellier, France. [5]Smithsonian Environmental Research Center, Edgewater, MD, USA. [6]Facultad de Ciencias Forestales, Universidad Juárez del Estado de Durango, Durango, Mexico. [7]Instituto de Silvicultura e Industria de la Madera, Universidad Juárez del Estado de Durango, Durango, Mexico. [8]Environmental and Rural Science, University of New England, Armidale, New South Wales, Australia. [9]Agence Nationale des Parcs Nationaux, Libreville, Gabon. [10]Ministère des Eaux, des Forêts, de la Mer et de L'Environnement, Libreville, Gabon. [11]Smithsonian Tropical Research Institute, Panama City, Republic of Panama. [12]Department of Plant Biology, University of Illinois, Urbana, IL, USA. [13]National Institute of Amazonian Research—INPA, Manaus, Brazil. [14]Programa Ciencias Básicas de la Biodiversidad, Instituto de Investigación de Recursos Biológicos Alexander von Humboldt, Bogotá, Colombia. [15]Departamento de Biología, Universidad Nacional de Colombia, Bogotá, Colombia. [16]Laboratório de Ecologia Vegetal (LABEV), Universidade do Estado de Mato Grosso, Nova Xavantina, Brazil. [17]Embrapa Amazônia Oriental, Belém, Brazil. [18]Living Earth Collaborative, Washington University in St. Louis, St. Louis, MO, USA. [19]Center for Conservation and Sustainable Development, Missouri Botanical Garden, St. Louis, MO, USA. [20]Herbario Vargas (CUZ), Escuela Profesional de Biología, Universidad Nacional de San Antonio Abad del Cusco, Cusco, Peru. [21]College of Life Sciences, University of Exeter, Exeter, UK. [22]Institut de Recherche en Écologie Tropicale, Libreville, Gabon. [23]Biological and Environmental Sciences, University of Stirling, Stirling, UK. [24]Center for Global Discovery and Conservation Science, Arizona State University, Tempe, AZ, USA. [25]Department of Biology, Sonoma State University, Rohnert Park, CA, USA. [26]School of Biological Sciences, University of Aberdeen, Aberdeen, UK. [27]College of Science and Engineering, James Cook University, Cairns, Queensland, Australia. [28]Department of Ecology and Evolutionary Biology, University of Arizona, Tucson, AZ, USA. [29]Department of Life Sciences, Imperial College London, Ascot, UK. [30]MCT/Museu Paraense Emílio Goeldi, Belém, Brazil. [31]Instituto de Biologia, Departamento de Biologia Vegetal, Universidade Estadual de Campinas, Campinas, Brazil. [32]Ecology and Global Change, School of Geography, University of Leeds, Leeds, UK. [33]Department of Geography, University College London, London, UK. [34]Coordenação de Dinâmica Ambiental, Instituto Nacional de Pesquisas da Amazônia, Manaus, Brazil. [35]Institute for Biodiversity and Ecosystem Dynamics (IBED), University of Amsterdam, Amsterdam, the Netherlands. [36]Department of Biology, Wake Forest University, Winston-Salem, NC, USA. [37]School of Natural and Environmental Sciences, Newcastle University, Newcastle Upon Tyne, UK. [38]Instituto de la Naturaleza, Tierra y Energía, Pontificia Universidad Católica del Perú, Lima, Peru. [39]Department of Plant Sciences and Conservation Research Institute, University of Cambridge, Cambridge, UK. [40]CSIR-Forestry Research Institute of Ghana, Kumasi, Ghana. ✉e-mail: jesus.aguirregutierrez@ouce.ox.ac.uk

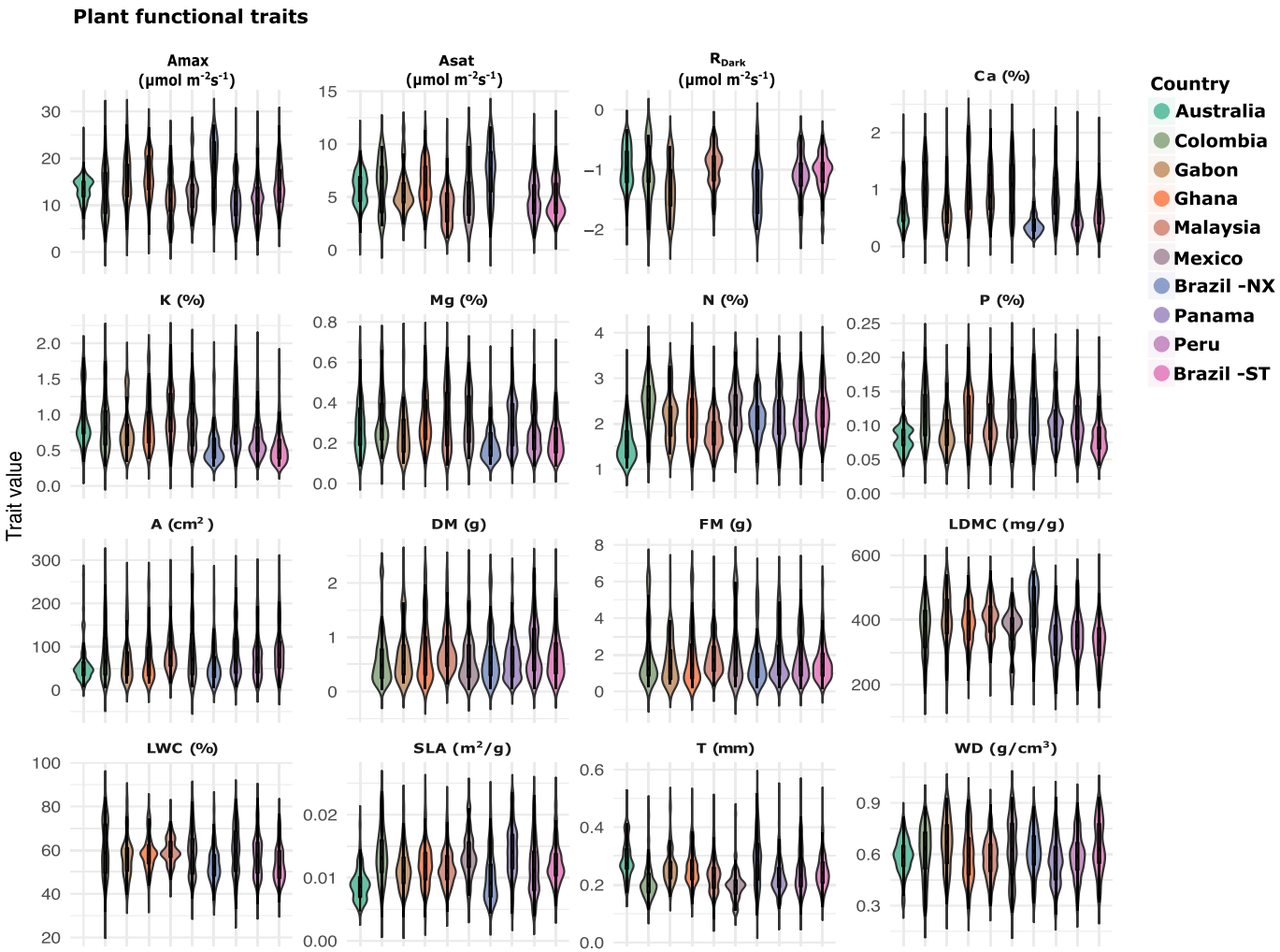

Extended Data Fig. 1 | Violin plots of the plant functional traits and their value ranges across the study area. The plant functional traits used in the study with raw trait values are shown (corresponding to $n = 2461$ individual trees) but these data were log-transformed prior to further analysis. The colours correspond to the field sampling areas where in situ traits collection plots are located; the Y axis shows the raw data values for each functional trait. Photosynthetic traits are A_{max}: Light-saturated maximum rates of net photosynthesis at saturated CO_2 (2000 ppm CO_2); μmol m^{-2} s^{-1}), A_{sat}: light-saturated rates of net photosynthesis at ambient CO_2 concentration (400 ppm CO_2; μmol m^{-2} s^{-1}), R_{Dark}: dark respiration (μmol m^{-2} s^{-1}). Leaf nutrient concentration traits are, Ca: leaf calcium (%), K: leaf potassium (%), Mg: leaf magnesium (%), N: leaf nitrogen (%), P: leaf phosphorus (%). Leaf morphological and structural traits are, A: leaf area (cm^2), DM: leaf dry mass (g), FM: leaf fresh mass (g), LDMC: leaf dry matter content (mg/g), LWC: leaf water content (%), SLA: specific leaf area (m2/g), T: leaf thickness (mm), WD: wood density (g/cm^3). No traits were collected in Mexico and were thus assigned to the vegetation censuses from other locations as explained in the methods section. Brazil -ST: Brazil Santarem, Brazil -NX: Brazil Nova Xavantina. The horizontal lines within each boxplot represent the mean trait value and the vertical lines encompass the first (25^{th}) and third (75^{th}) quartiles of the data distribution for each trait.

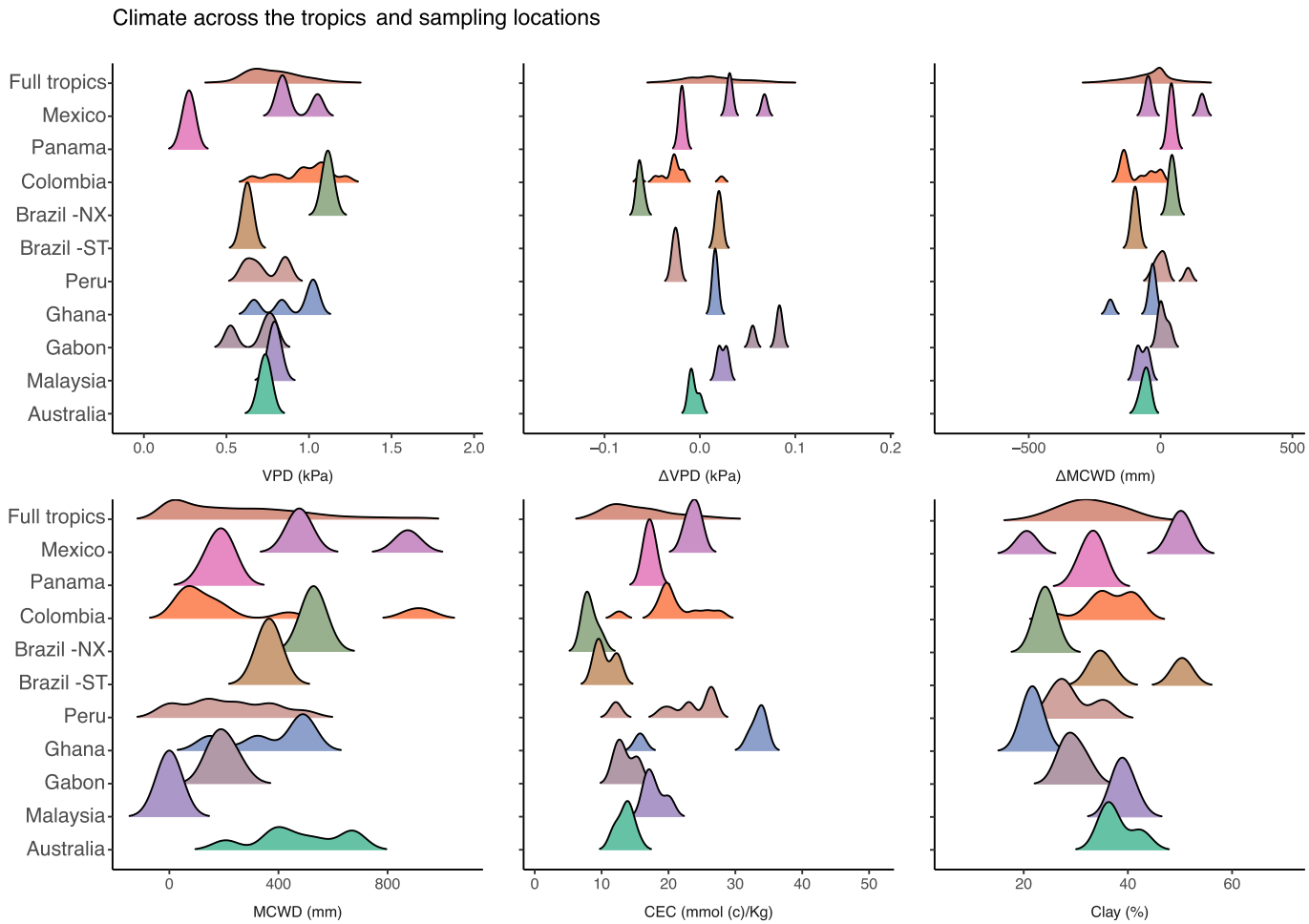

Extended Data Fig. 2 | Density plots of the climatic and soil conditions that encompass each field sampling location where plant functional traits and vegetation censuses were collected. The top density graph of each climatic and soil variable shows the values found across the tropical and subtropical dry and moist broadleaf forests. VPD: vapour pressure deficit, MCWD: maximum climatic water deficit, CEC: cation exchange capacity, Δ: change.

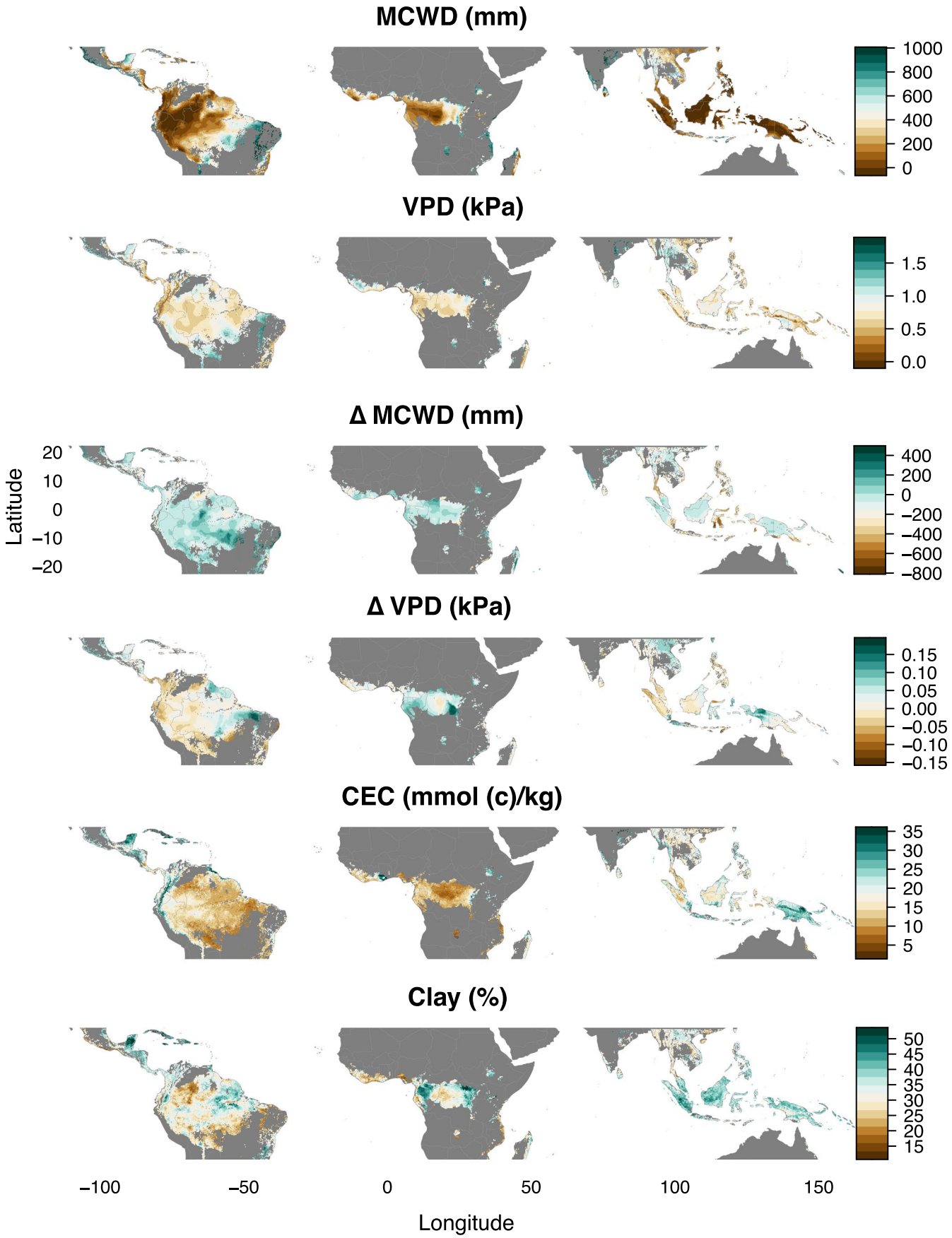

Extended Data Fig. 3 | Spatial distribution of climatic and soil conditions across the tropical and subtropical dry and moist broadleaf forests. MCWD: maximum climatic water deficit, VPD: vapour pressure deficit, CEC: soil cation exchange capacity, Clay: soil clay content. Δ: change.

a) PCA of sampling locations in climate space

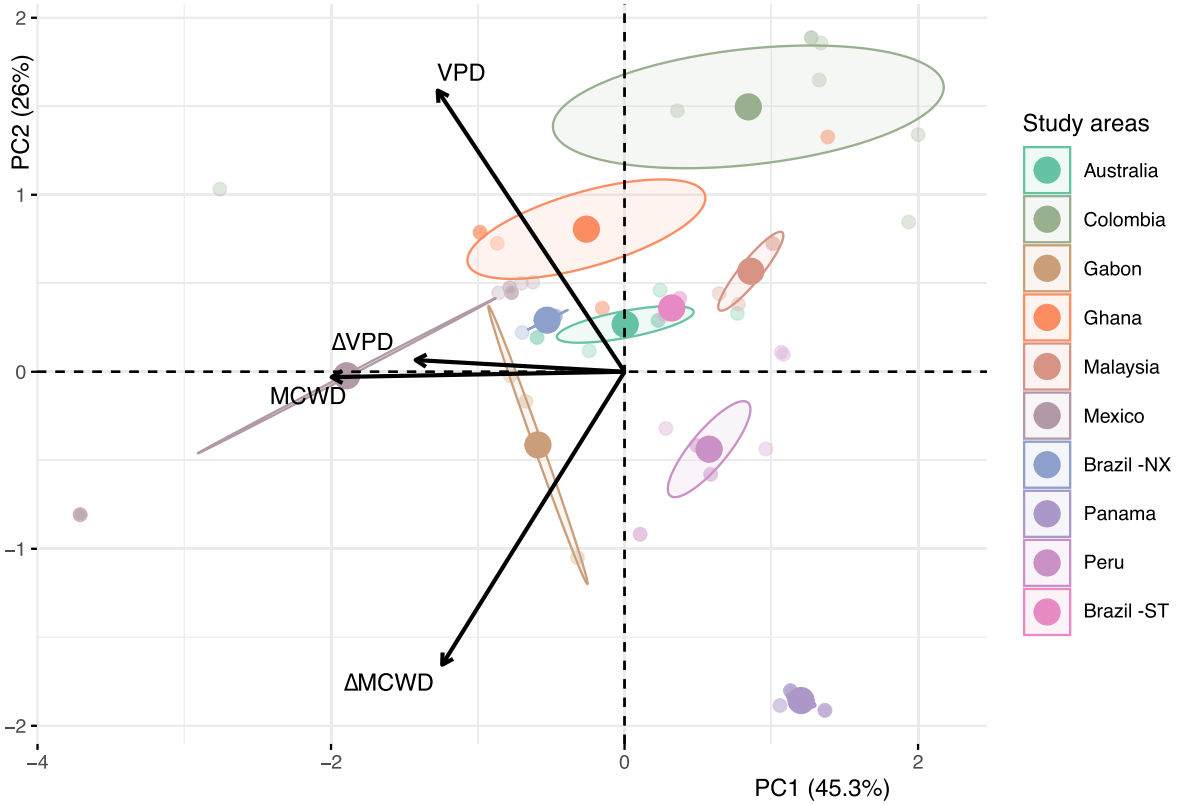

b) PCA of sampling locations according to soil characteristics

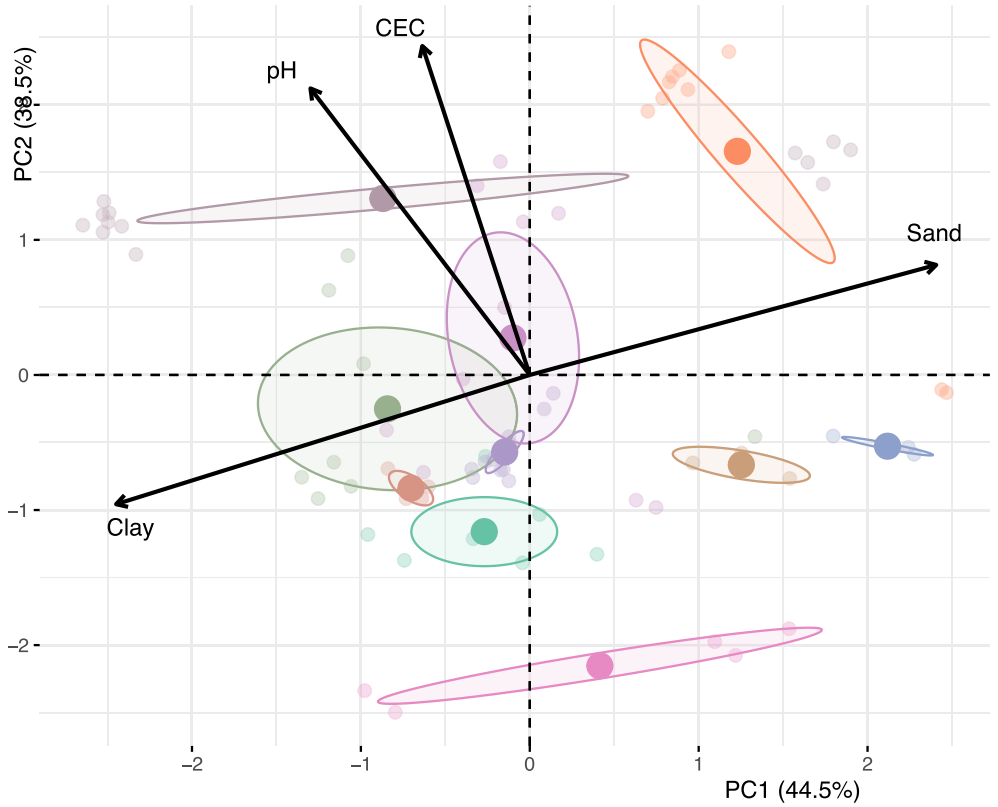

Extended Data Fig. 4 | See next page for caption.

Extended Data Fig. 4 | Principal component analysis of the distribution of the plot locations in environmental space. The PCA in (a) shows the distribution of plots in climatic and (b) in soil space. MCWD: average Maximum Climatic Water Deficit and VPD: average Vapour Pressure Deficit, ΔMCWD and ΔVPD: change in MCWD and VPD respectively between the 1958–1987 and 1988–2017 period. MCWD and VPD represent the full-term climatic conditions (1958–2017 period). CEC: cation exchange capacity and soil pH are highly correlated and only CEC is used for further analysis. Clay and sand are highly correlated and only clay is used for further analysis. Coloured ellipsoids in a) and b) encompass 95% of the distribution of the vegetation plots from each field sampling location.

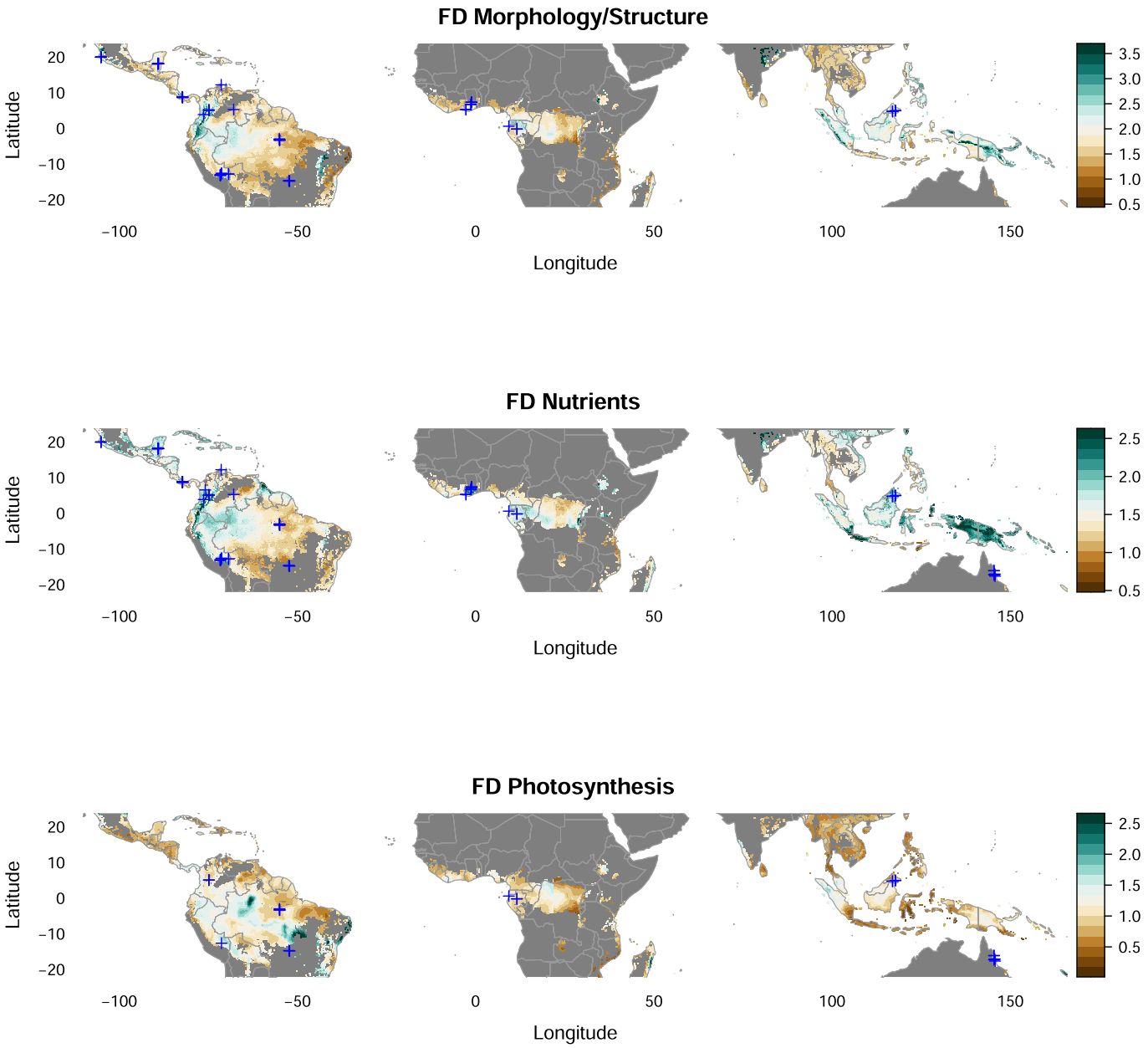

Extended Data Fig. 5 | Spatial predictions of functional diversity (FD) depicting the locations of vegetation plots (blue crosses) that were used to fit the statistical models. The spatial predictions of morphological/structural (top panel), nutrients (middle panel) and photosynthetic (bottom panel) traits are shown. For details about the plots, their location and climatic and soil conditions see Supplementary Table S1).

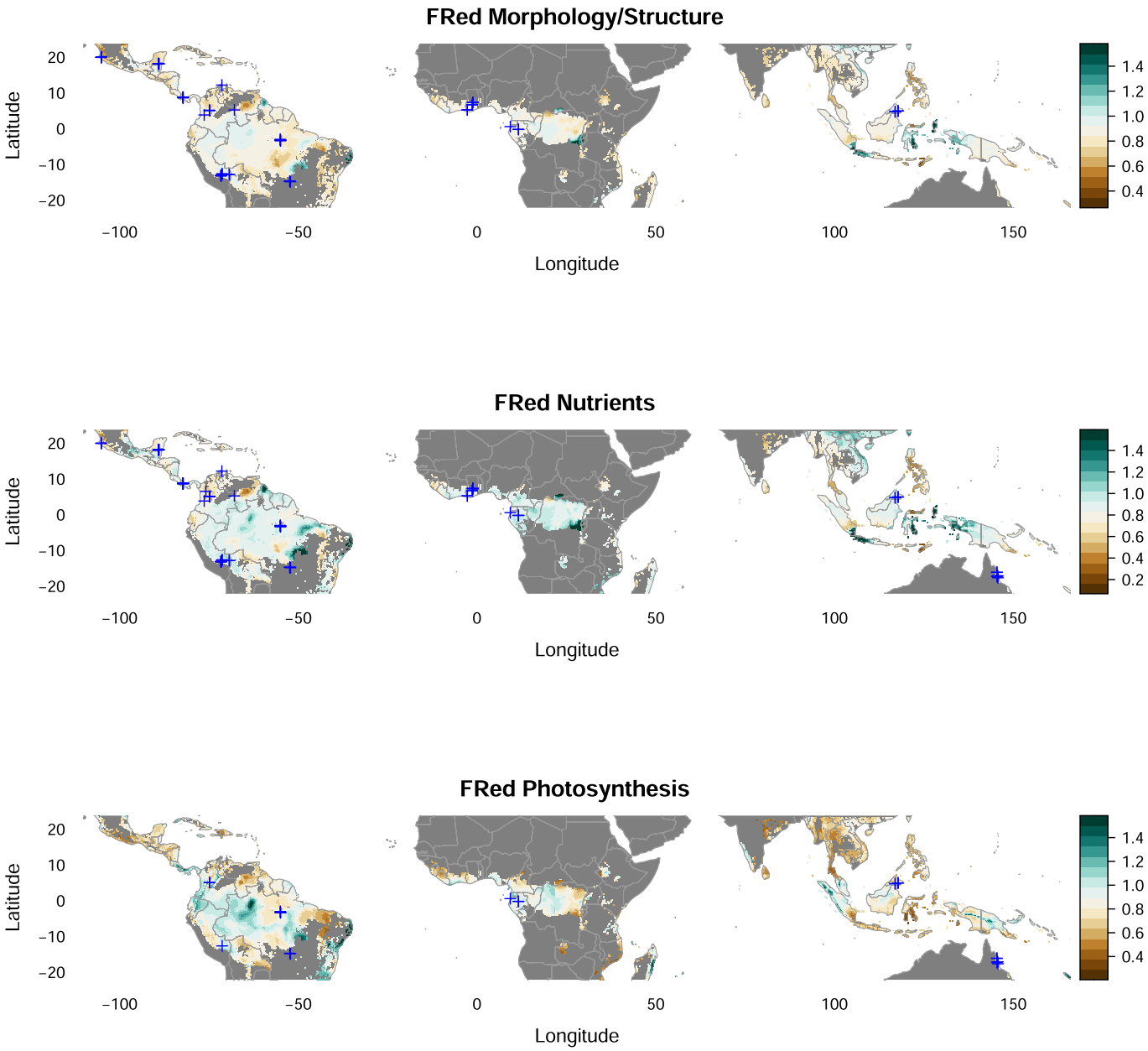

Extended Data Fig. 6 | Spatial predictions of functional redundancy (FRed) depicting the locations of vegetation plots (blue crosses) that were used to fit the statistical models. The spatial predictions of morphological/structural (top panel), nutrients (middle panel) and photosynthetic (bottom panel) traits are shown. For details about the plots, their location and climatic and soil conditions see Supplementary Table S1).

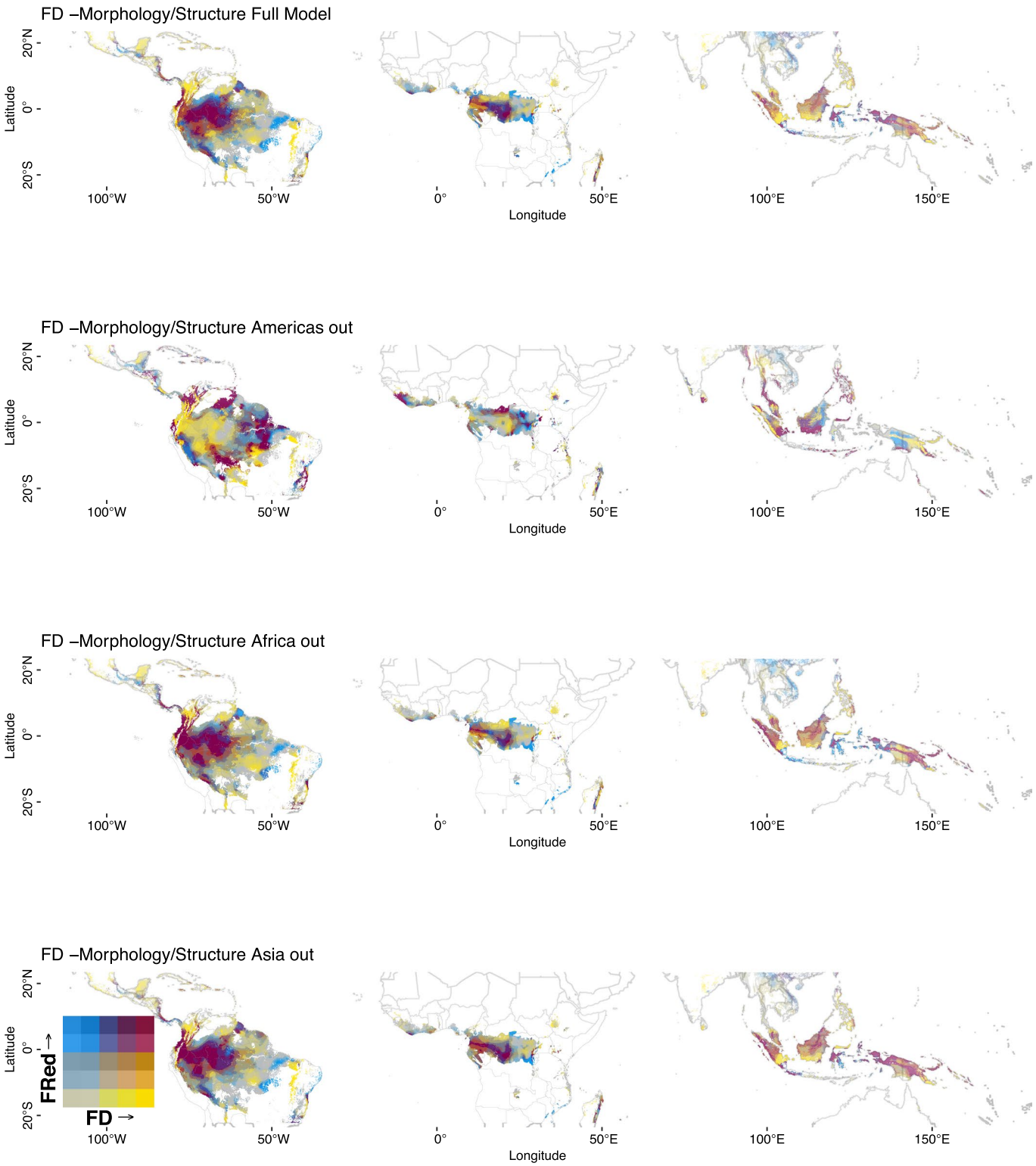

Extended Data Fig. 7 | Bivariate maps combining the functional diversity (FD) and redundancy (FRed) for the morphological traits. Each map shows the predictions obtained using the full dataset (full model, top panel) and the changes that occur by leaving the plots from each continent out of the model. The second panel shows the spatial predictions when leaving the records from the Americas out of model fitting, the third panel when leaving records from Africa out and the bottom panel when leaving the records from Asia and Australia out from model fitting.

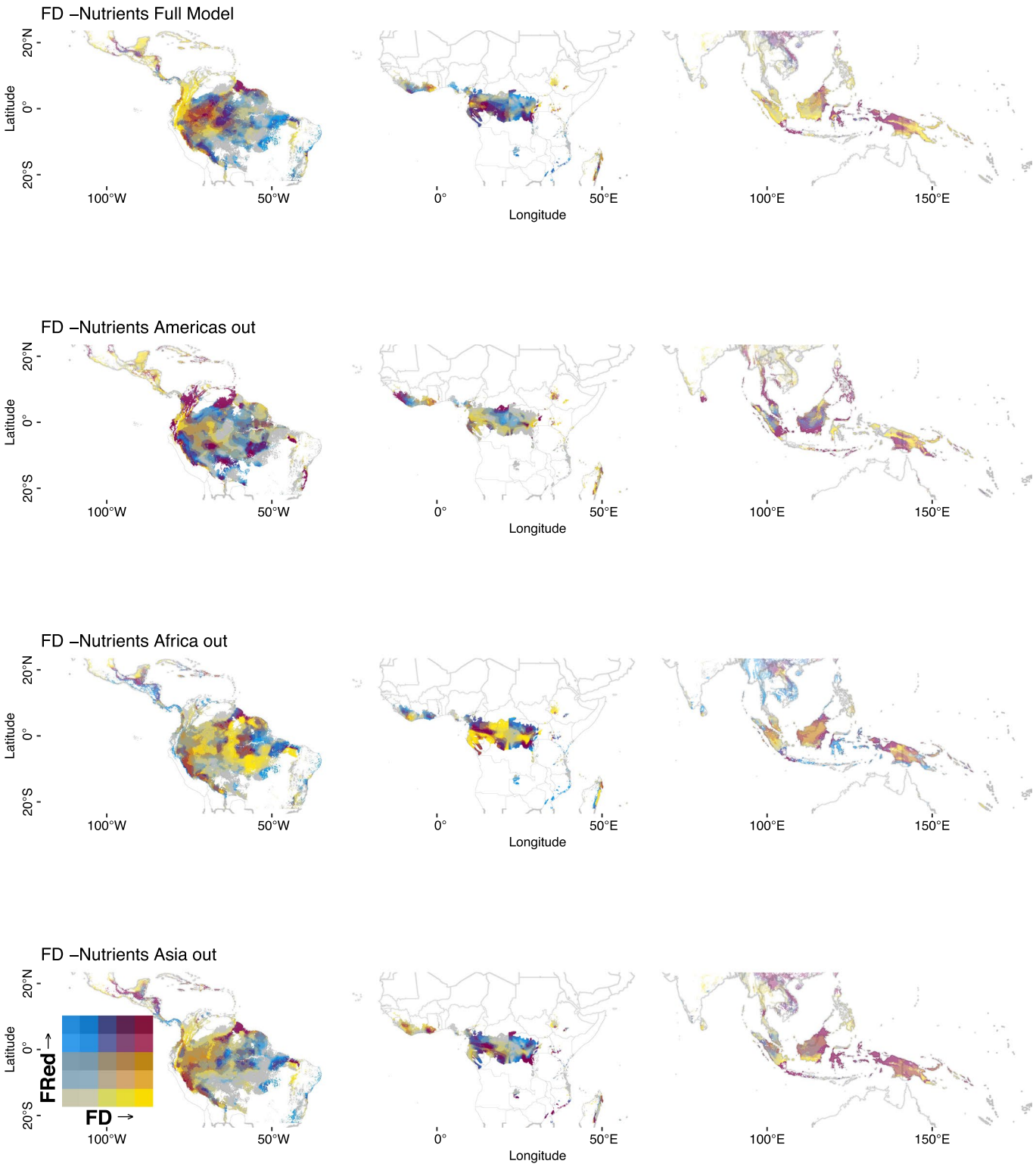

Extended Data Fig. 8 | Bivariate maps combining the functional diversity (FD) and redundancy (FRed) for the nutrients traits. Each map shows the predictions obtained using the full dataset (Full model) and the changes that occur by leaving the plots from each continent out of the model. The second panel shows the spatial predictions when leaving the records from the Americas out of model fitting, the third panel when leaving records from Africa out and the bottom panel when leaving the records from Asia and Australia out from model fitting.

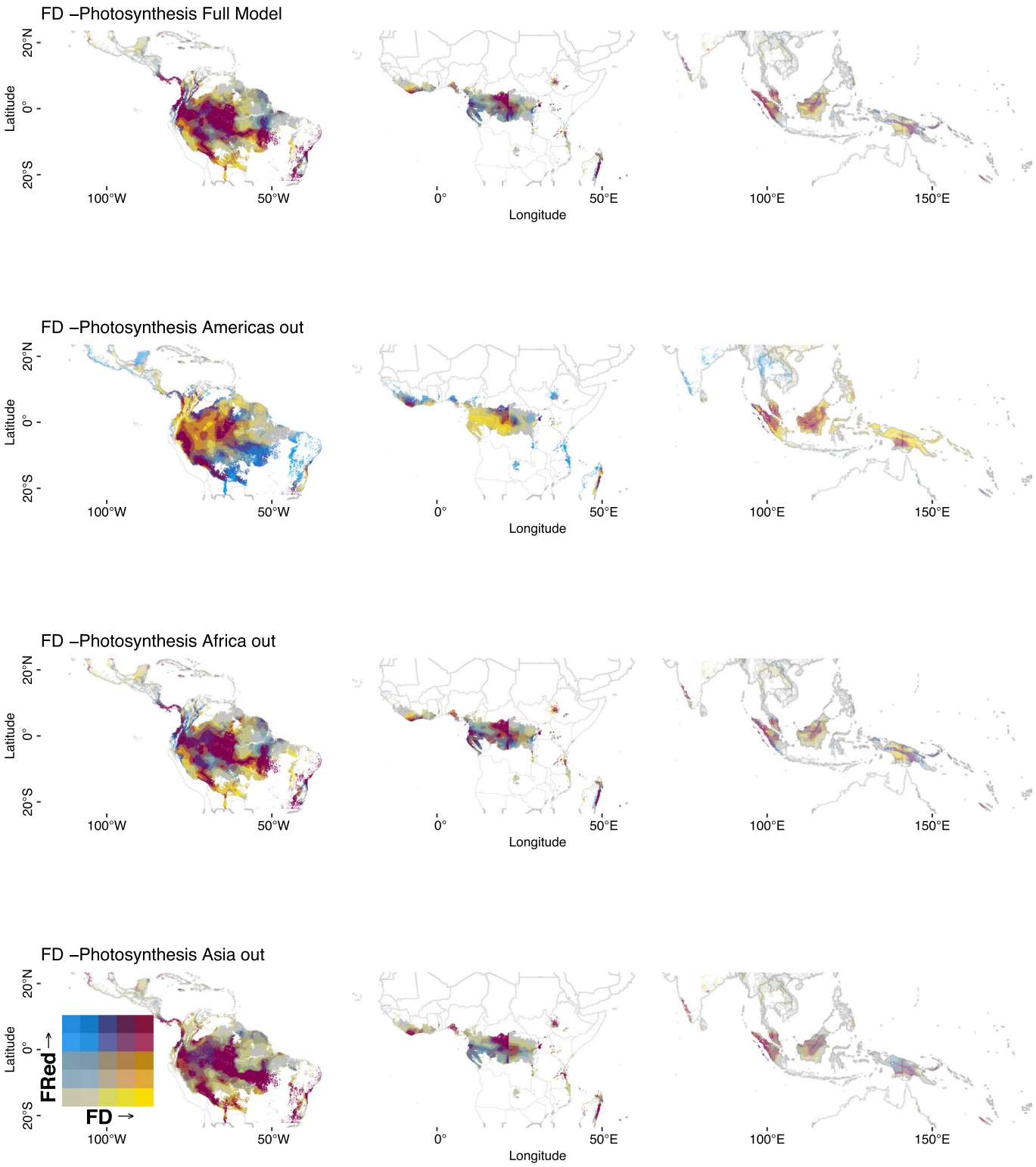

Extended Data Fig. 9 | Bivariate maps combining the functional diversity (FD) and redundancy (FRed) for the photosynthesis traits. Each map shows the predictions obtained using the full dataset (Full model) and the changes that occur by leaving the plots from each continent out of the model. The second panel shows the spatial predictions when leaving the records from the Americas out of model fitting, the third panel when leaving records from Africa out and the bottom panel when leaving the records from Asia and Australia out from model fitting.

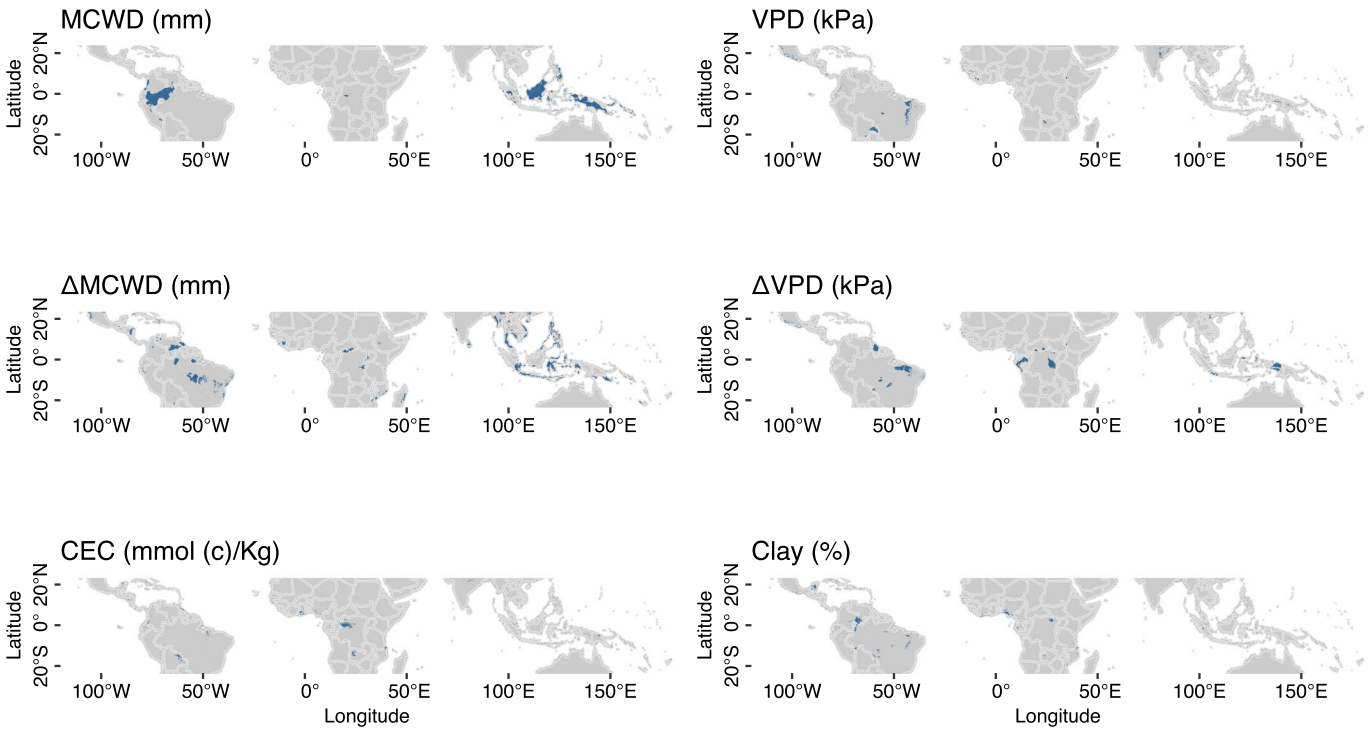

Extended Data Fig. 10 | Distribution of locations that contain climatic and soil values out of the range used to fit the statistical models of functional diversity (FD) and functional redundancy (FRed). The results of FD and FRed scores for those areas (in blue) should be interpreted with caution. See Fig. 3 and Fig. 4 for the FD and FRed spatial predictions. MCWD: maximum climatic water deficit, VPD: vapour pressure deficit, CEC: soil cation exchange capacity, Clay: soil clay content. Δ: change.